Urban building energy modelling and multi-objective optimization for PED transition in an existing neighbourhood in Sweden

Energy & Buildings 352 (2026) 116783

Contents lists available at ScienceDirect

Energy & Buildings

journal homepage: www.elsevier.com/locate/enbuild

Urban building energy modelling and multi-objective optimization for PED transition in an existing neighbourhood in Sweden

Sara Abouebeid [a,*], Jenny Enerbäck [b], Elena Malakhatka [a], Ann-Brith Strömberg [b], David Sindelar [a], Mohammadreza Mazidi [c], Araavind Sridha [c], Holger Wallbaum [a], Liane Thuvander [a]

[a] Department of Architecture and Civil Engineering, Chalmers University of Technology, Gothenburg, Sweden
[b] Department of Mathematical Sciences, Chalmers University of Technology and University of Gothenburg, Gothenburg, Sweden
[c] Department of Electrical Engineering, Chalmers University of Technology, Gothenburg, Sweden

ARTICLE INFO

Keywords:
Urban building energy modelling
Positive energy districts
Multi-objective integer linear optimization
Renewable energy
Energy efficiency

ABSTRACT

Transitioning existing urban neighbourhoods to Positive Energy Districts (PEDs) requires integrated planning to address complex energy, cost, and lifecycle carbon emission challenges. Existing integrated methodologies optimize buildings individually and overlook local energy systems potentials like shared renewables and battery storage. Moreover, existing studies on optimization of on-site renewable energy sources and building retrofitting often rely on simplified typical-day representations, falling short in capturing critical operational dynamics over tim0e. This paper introduces and applies an integrated urban building energy modelling and bi-objective mixed-integer linear programming framework. The framework co-optimizes building retrofits and heating systems, PhotoVoltaic (PV) systems, and Battery Energy Storage System (BESS) capacities over a 10-year horizon with hourly resolution, targeting minimal lifecycle costs and total carbon emissions (operational and embodied).

Applied to a 1950s neighbourhood in Gothenburg, Sweden, the analysis demonstrated that achieving full PED status (net-zero energy import, net-zero carbon, and energy surplus) with the evaluated interventions is highly challenging. While optimized solutions reduced the grid dependency (to ~63 % with PV and BESS under volatile prices) and overall carbon emissions (by ~13 % compared to baseline), neither complete net-zero energy import, full carbon neutrality including embodied impacts, nor an energy surplus were realized. The study quantitatively identified critical trade-offs between investment costs, embodied carbon, operational performance, and resilience. Optimal solutions were sensitive to local conditions, notably low-carbon district heating and electricity price volatility. The proposed framework provides a decision-support tool for strategic PED planning in existing urban areas, enabling an exploration of complex techno-economic and environmental trade-offs.

1. Introduction

Cities are pivotal in the global energy transition, accounting for around two-thirds of the world's primary energy consumption and 75 % of energy-related greenhouse gas emissions [1]. Being densely populated hubs of diverse activities [2], cities' effective decarbonization is crucial for meeting the climate mitigation targets outlined in the Paris Agreement [3]. While concepts like Net Zero Energy Buildings and Net Zero Energy Districts have marked progress [4–6], the Positive Energy District (PED) concept has emerged as a more ambitious paradigm. Traditionally, PEDs are defined as districts achieving net-zero or surplus annual energy production through an extensive integration of Renewable Energy Sources (RES), high energy efficiency, and smart energy flexibility strategies [7–10].

Adopting a district-scale lens is critical to unlocking synergies—such as thermal load diversity enabling efficient district energy systems, RES integration, energy flexibility, and shared electric vehicle charging infrastructure interacting with local grids—, which are fundamentally obscured by a building-centric view [11]. This shift has led to the development of the PED concept—an approach that aims for districts to achieve annual net-zero energy imports and carbon emissions, while ultimately generating a surplus of locally produced renewable energy [7].

Despite dedicated research on building retrofitting [12,13] and urban RES deployment [14], a critical research gap persists: there is a lack of validated, integrated methodologies specifically designed to plan, optimize, and assess PED transformation pathways within the complex constraints of existing urban districts [15]. Fragmented or purely

* Corresponding author.
E-mail address: saraabo@chalmers.se (S. Abouebeid).

https://doi.org/10.1016/j.enbuild.2025.116783
Received 20 May 2025; Received in revised form 3 November 2025; Accepted 24 November 2025
Available online 28 November 2025

Nomenclature

ASHP	Air Source Heat Pump
BESS	Battery Energy Storage System
BIPV	Building Integrated PhotoVoltaic
DHS	District Heating System
DOE	U.S. Department Of Energy
DTCC	Digital Twin Cities Centre
EPBD	EU Energy Performance of Buildings Directive
EPC	Energy Performance Certificate
EPDM	Ethylene Propylene Diene Monomer
EPS	Expanded Polystyrene
FCS	Future Climate Scenario
GIS	Geographical Information System
GSHP	Ground Source Heat Pump
GWP	Global Warming Potential
HVAC	Heating, Ventilation, and Air Conditioning
ICT	Information and Communication Technology
KPI	Key Performance Indicator
MAPE	Mean Absolute Percentage Error
MILP	Mixed-Integer Linear Programming
MIT	Massachusetts Institute of Technology
OSB	Oriented Strand Board
PED	Positive Energy District
PIR	Polyisocyanurate
PV	PhotoVoltaic
PVGIS	PhotoVoltaic Geographical Information System
RCP	Representative Concentration Pathway
RES	Renewable Energy Sources
RP	Retrofit Package
Setup 2022	A volatile electricity spot price scenario, from 2022
Setup 2023	A more stable electricity spot price scenario, from 2023
TMY	Typical Meteorological Year
UBEM	Urban Building Energy Modelling

sequential planning often fails to capture the interplay between demand reduction measures (i.e., retrofit strategies including lifecycle-wide carbon emissions), on-site RES generation, energy storage, and system-wide operational dynamics, thereby missing techno-economic synergie [14].

While some electricity system investment models account for long-term planning horizons and high temporal resolution [16], studies focused on optimizing on-site RES and building retrofitting often rely on shorter planning periods or simplified typical-day representations [17–19]. As a result, they fall short in capturing critical operational dynamics over time, such as investment capacity degradation, fluctuating electricity prices, and the temporal behavior of energy storage systems.

These limitations in current modelling practices—fragmented planning approaches, restricted temporal horizons, and lack of integration of retrofit and RES strategies—underscore the importance of place-specific strategies that respond to local energy contexts, infrastructure, and planning traditions. In this regard, Sweden offers a compelling case study due to its progressive climate goals and energy system characteristics.

Sweden's national energy context significantly shapes the opportunities and challenges for implementing PEDs. The country is a recognized global leader in climate action, pursuing ambitious targets including net-zero carbon emissions by 2045 and pioneering market mechanisms like the world's highest carbon price. This commitment is reflected in its electricity generation, which is over 96 % derived from fossil free sources, predominantly hydropower (~40 %), nuclear power (~30 %), and a growing share of wind power (~25 %). With more than 96 % of electricity generated from fossil-free sources, the Swedish energy system is already low-carbon, creating challenges that differ from those in regions where grid decarbonization remains the primary goal.

Recognizing this advanced baseline, this study adopts the JPI Urban Europe definition [8] of a PED as "an energy-efficient urban neighbourhood that generates a local surplus of renewable energy, achieves net-zero greenhouse gas emissions annually, and actively integrates with regional energy, mobility, and ICT systems to support broader climate-neutrality goals", as a conceptual starting point. An additional target is introduced: a climate-positive district ambition that accounts for both operational and embodied carbon emissions, capturing the greenhouse gases associated with energy use during building operation and with the production and installation of building materials (A1–A3 and B6 according to EN 15978 [20]), recognizing that in a low-carbon electricity system, material-related emissions represent a growing share of total climate impact.

The heating sector, particularly in urban areas, relies on District Heating System (DHS) networks, often utilizing bio-energy sources like forestry residues and waste heat recovered from industries or data centers [21]. Solar energy currently plays a minor role, accounting for only around 1 % of generation [22]. Moreover, Sweden presents specific advantages for PhotoVoltaic (PV) systems: cooler ambient temperatures boost panel efficiency, and the low-angle solar radiation benefits vertical PV installations, aiding self-consumption and peak shaving. Therefore, designing effective PEDs in Sweden requires careful consideration of these factors: leveraging the low-carbon electricity grid, improving the existing DHS infrastructure, and strategically deploying solar PV, acknowledging both its potential and its current limitations. Hence, the study addresses the following overarching research question: How can an integrated Urban Building Energy Modelling (UBEM) and Mixed-Integer Linear Programming (MILP) framework be developed and applied to co-optimize building retrofits, on-site renewable energy generation, and shared energy storage over a long-term horizon, in order to minimize lifecycle costs and carbon emissions while guiding the transformation of existing urban neighbourhoods toward a PED status?

To address this research question, this study develops and demonstrates an integrated framework combining UBEM with a bi-objective MILP model for optimizing the transition of existing neighbourhoods into PEDs. The primary contribution of this research lies in the establishment of a robust and replicable methodology that

1. employs a detailed, calibrated UBEM to accurately assess baseline energy performance, evaluate a wide array of building retrofit packages (considering material properties in terms of their impact on heating demand, embodied carbon, and material cost), and quantify the on-site solar PV potential within an existing neighbourhood;
2. integrates these detailed UBEM simulation outputs into a strategic MILP model designed for long-term (10-year) investment planning with a high temporal (hourly) resolution. This model co-optimizes the selection of retrofit packages, the capacities of PV systems, and Battery Energy Storage System (BESS) to minimize the total lifecycle costs and carbon emissions (embodied as well as operational).

Our integrated framework provides an advancement by offering a decision-support tool capable of navigating the complexity of a simultaneous optimization of retrofitting strategies and RES integration in established urban areas. The efficacy of the proposed framework is demonstrated through its application to the Jättesten neighbourhood in Gothenburg, Sweden—a typical mixed-use area with mid-20th-century building stock. Our case study provides concrete insights into the techno-economic and environmental trade-offs involved in pursuing PED targets within the specific context of Sweden's low-carbon energy system.

2. Background and related theory

2.1. Building retrofit and neighbourhood energy planning

The transformation of existing buildings into PEDs presents significant challenges, not only due to their generally poor energy

performance (e.g., [23]), but also because of the complex, context-specific constraints that shape retrofit decisions. Existing infrastructure—such as district heating networks or aging electric grid—can limit the feasibility or cost-effectiveness of certain measures. Buildings also vary widely in condition, meaning they do not all require the same level or timing of renovation. Moreover, districts often include a mix of residential and non-residential buildings, such as educational and commercial facilities, each with different ownership structures and renovation priorities. This diversity complicates coordinated interventions and requires flexible, targeted strategies that reflect the technical, functional, and institutional realities of the built environment.

Poor insulation remains one of the greatest challenges in the European building stock, with an estimated 35 million buildings (2012/27/EU) classified as energy inefficient due to inadequate thermal performance; Mangold, Mikael [23]. The EU Directive on the Energy Performance of Buildings (2002/91/EU; 2010/31/EU–EPBD; EU/2024/1275) emphasizes an improvement of the energy performance of existing buildings and advocates deep renovations; Erba and Pagliano [24], D'Oca et al. [25].

The term "retrofit" denotes processes involving the renovation, modification, or enhancement of existing buildings, aimed at updating their components and systems to align with contemporary standards and functional requirements. These interventions also serve to extend the buildings' service life and overall performance; Citadini De Oliveira et al. [12]. Compared to demolition and reconstruction, retrofitting offers notable economic, social, and environmental advantages; Citadini De Oliveira et al. [12], Langston [26] including reduced waste generation, lower consumption of natural resources and preserving cultural values. As a result, retrofitting existing buildings contributes to reducing energy consumption and greenhouse gas emissions, thereby supporting the transition toward a more sustainable built environment.

Evidence from recent Swedish studies [27] underscores the dual challenge of achieving deep energy retrofits and PED targets while safeguarding indoor comfort in a warming climate; it is shown that even deep envelope upgrades can lower heating demand by more than 70 % but have only a modest impact on future cooling loads, which are projected to increase up to six-fold by 2080 in the most severe climate pathway. A detailed assessment of passive cooling strategies in a renovated multi-family building in Gothenburg [28] further indicates that annual cooling demand of only 0.46 kWh/m^2 in 2018 is expected to rise by 180–230 % by 2030 and by 280–400 % by 2050 (to 1.3–1.9 kWh/m^2) under RCP4.5 and RCP8.5 (Representative Concentration Pathways; Riahi [29]) with peak cooling demand increasing by up to 98 %. Overheating hours already exceed the 10 % comfort threshold and could reach 38 % by 2050 without additional measures.

In addition, several countries are increasingly concerned about the affordability of retrofitting and energy conservation measures; Ma'bdeh et al. [30]. Numerous studies have highlighted the economic barriers to such activities (e.g., [31,32]), with evidence that energy retrofitting can also lead to socio-economic drawbacks, particularly increased rents and housing costs [32–34].

2.2. Renewable energy sources (RES) integration

The concept of PEDs is fundamentally tied to the widespread use of RES. The goal is to go beyond net-zero energy and achieve an annual energy surplus, primarily from locally generated renewable energy. In urban areas, solar PV technology is essential and effective strategies require deploying PV at multiple scales, from individual buildings to entire district energy systems. The effectiveness of these systems depends on several geometric and environmental factors, such as available surface area, orientation and tilt, incoming solar radiation, and importantly, shading from nearby buildings and vegetation within the urban setting. Although solar energy has historically played a limited role in Sweden, PV technology offers favourable operational benefits there, such as lower ambient temperatures. Therefore, strategic and well-planned PV deployment is considered crucial for developing successful PEDs in Sweden. District-level PV deployment involves collective renewable energy generation and shared infrastructure, which supports more comprehensive energy ecosystems. Important technical and economic benefits can be achieved by combining PV with energy storage, particularly BESS, through which the misalignment of peaks of electricity demand and electricity production can be bridged. This helps maximize the use of self-generated solar power, increases energy flexibility, and improves system resilience, especially when electricity market prices fluctuate.

However, implementing PV and other RES technologies in existing urban districts presents significant challenges. These challenges include the difficulties of working with established urban areas, like limited space for new installations, a lack of validated, integrated methods for comprehensive planning and optimization and tax system [35,36]. As a result, accurately quantifying PV potential is essential. and it is increasingly being done using advanced computational tools like UBEM and specialized solar analysis software [35,36]. These assessments are vital for PED planning and for realistically evaluating the ability to achieve energy self-sufficiency.

2.3. Urban building energy modelling (UBEM) approaches in PED planning

As cities aim to decarbonize and increase resilience, UBEM has become a crucial method for assessing district-scale energy performance and for guiding PED development. Unlike conventional single-building simulations, UBEM captures the interdependence through feedback loops between multiple buildings, heating and electricity infrastructure, and their surrounding urban context.

UBEM is classified into two main categories of modelling approaches: top–down and bottom–up [37]. Top–down models utilize aggregated historical data to estimate building performance through correlations between energy consumption and various socio-economic, technical, and physical parameters [37,38]. Top–down models are typically more suitable for early-stage planning, where broad energy consumption trends are analysed at a high level to inform strategic decisions. Conversely, bottom–up models employ detailed, physics-based simulations at a disaggregated level, being valuable during the operation phase and offering richer insights into nuances of retrofit planning for individual buildings [39]. Their advantage lies in detailed energy flow representations that integrate multiple external influencing factors, enabling analysis across varying temporal resolutions unique to each building. By incorporating time-varying schedules and dynamic loads, bottom–up approaches allow for high-resolution simulations (e.g., hourly), which are essential for accurately capturing variations throughout the day in energy demand and supply. This study focuses on the bottom–up approach.

Datasets required for bottom–up modelling include building characteristics—e.g., geometry, material thermal properties—, energy systems—e.g., Heating, Ventilation and Air Conditioning (HVAC) systems, lighting, and appliances—, occupancy schedules, and internal loads [37,40–42]. These data types typically fall into geometric and semantic categories but frequently originate from fragmented sources, including national databases, Energy Performance Certificates (EPCs), and metering records. Previous studies [43] have investigated how elements of the urban context—such as neighbouring buildings [44], vegetation [45], and other urban systems [46]—affect thermal and electricity demands [47–49].

Various UBEM tools have been developed to assess energy efficiency and flexibility in PEDs. Tools like EnergyPlus [50,51], Ladybug Tools [52], and UrbanOpt [53,54] have been widely applied in this context. These tools compute a range of energy-related metrics, such as energy demand, renewable energy generation, and overall energy balance, for buildings interconnected with urban infrastructures such as district heating and cooling systems. These metrics serve as key performance indicators (KPIs) for evaluating PEDs' energy performance. Additionally, UBEM tools are capable of computing carbon emissions, climate and thermal comfort KPIs, supporting a multi-dimensional assessment

of PED performance. However, these tools differ significantly in spatial-scale modelling, computational complexity, and output resolution, influencing their applicability for different PED criteria.

In summary, the existing frameworks lack two key areas as they have a narrow focus on envelope configurations and excluding lifecycle perspectives of environmental impacts. In a review of 54 UBEM studies published between 2001 and 2022, [55] found that most applications focus on single-envelope configurations, typically analyzing only wall structures and deriving thermophysical properties from window-to-wall ratios while neglecting thermal bridging and multi-component effects [56]. Furthermore, earlier studies predominantly report energy-related outputs such as electricity consumption, heating demand, or energy use intensity, without incorporating lifecycle assessment approaches that consider the full environmental impact of interventions over time.

2.4. Optimization models

MILP modelling combined with mathematical optimization algorithms provides an effective tool for identifying optimal or near-optimal solutions in a large solution space. It is used in many energy system planning applications to find optimal investments: Granfeldt et al. [16], Göransson et al. [57], Wirtz et al. [58], McCarty et al. [59], and can be adapted to large-scale problem instances, on the energy sector level [16,57], down to a local scale on the building/district level [17,19].

Models of investments in and operation of energy systems can be formulated as MILPs and are increasingly being used to find cost-minimizing decarbonization strategies for building energy systems [60]. To exploit the interrelatedness of the effects of investments on energy demand side (retrofitting) and investments in RES, many studies combine these two types of investments in a single optimization framework; e.g. [17–19,61,62].

These studies take different approaches regarding spatial resolution (single building or whole district), scheduling of investments (single- or multi-stage), and length of the planning period. The model presented in [19] allows for investments in retrofit packages and technical systems only at the beginning of the planning period, i.e., single-stage, and operations are optimized over a single representative year. Buildings are categorized based on age, size, and current retrofit state, and optimized separately for each category. The authors of [61] present a multi-stage optimization model in which investments can be made in several investment years, such that at the end of life of a technical component, a new investment can be chosen to retain the capacity, which is an improvement compared to the static investment planning of [19]. While [17,18] consider separate buildings for which investments and operation are optimized, [61] considers the simultaneous optimization over multiple buildings, that are connected through the possible expansion of a district heating system. The models consider planning horizons of up to 30 years; the computational complexity being reduced via the use of representative days for energy demands and solar radiation.

2.5. Research gap

The transition towards PEDs is a critical component of urban decarbonization strategies, and various facets of this transition have garnered considerable research attention. However, despite these advancements, several research gaps remain, particularly concerning the integrated and holistic planning of PED transformations within the complex fabric of existing urban neighbourhoods, where retrofitting the current building stock poses technical, financial, regulatory, and logistical challenges that are largely absent in purpose-built developments [63].

High initial costs and uncertain returns on investment create significant financial barriers, while regulatory constraints, such as building codes and zoning requirements, further complicate retrofitting efforts [64]. The potential disruption to occupants adds operational difficulties, and managing sustainable retrofitting projects is inherently complex, involving multiple stakeholders, intricate planning, and detailed execution [65]. Such projects require close collaboration among architects, engineers, contractors, and building owners, each with distinct priorities and challenges. Retrofitting also demands careful consideration of structural limitations; unforeseen issues such as hidden structural defects or outdated infrastructure often necessitate adjustments to the original plan [64]. Existing buildings may offer limited space for installing insulation or renewable-energy systems, and internal insulation can reduce usable floor area [66].

For optimization frameworks, there is a lack of methodologies to optimize PED transformations that exploit the environmental and economic advantages of local energy communities, enabled by shared BESS and transmission of locally produced electricity within the district. While some of the mentioned methodologies [17–19,61] combine, on district level, demand side interventions with RES deployment, their optimization models decouple to optimization of individual buildings due to the lack of interconnections between buildings (with the exception of [61], where buildings connect in the spatial dimension. through modeling of the expansion of district heating network). By not considering the interconnected operation of buildings, and therefore interconnected effects of investments, opportunities for holistic techno-economic and environmental optimization, in line with the idea of PED, are missed.

Further, existing optimization frameworks applied to PED planning frequently exhibit limitations in scope and resolution, particularly when addressing long-term investment horizons. Many models either focus on detailed building-level analysis with simplified district interactions or address district-level energy systems using aggregated building data, often neglecting the granular building-specific performance characteristics crucial for accurate retrofit and RES assessment. Additionally, most frameworks fail to optimize over a long planning horizon while maintaining a high temporal resolution—many papers use representative days which is not compatible with modelling of battery energy levels and does not account for fluctuations in energy demand and prices on a large scale.

Lastly, although multi-objective optimization is increasingly employed, there is a need for frameworks that more comprehensively integrate detailed lifecycle considerations for both costs and carbon emissions in the optimization process. This includes the embodied carbon associated with retrofit materials and energy system components, alongside operational carbon emissions. Simultaneously optimizing the selection of diverse retrofit packages, the sizing and placement of PV systems, and the capacity of BESS, while accounting for detailed lifecycle impacts and costs over a long planning period, remains a complex challenge that is not sufficiently addressed by current tools.

Hence, there is a need for an integrated decision-support framework bridging detailed, physics-based building energy modelling with district-scale multi-objective optimization. Such a framework should be capable of co-optimizing investments in building retrofits, renewable energy systems, and long-term energy storage with a fine temporal resolution. This study addresses this gap by developing and demonstrating an integrated UBEM–MILP methodology tailored for the strategic planning and evaluation of PED transformation pathways in existing urban neighbourhoods.

3. Methodology

3.1. Workflow

This study follows a three-step methodological workflow (see Fig. 1). The first step involves a comprehensive data collection, encompassing building attributes (e.g., geometry, use, orientation), baseline building energy performance data (e.g., electricity and heating demand), and economic and environmental data such as material prices, embodied carbon values, and renewable system costs. These datasets serve as the foundation for the UBEM setup, calibration, and optimization model.

The second step involves developing a district-scale UBEM using Rhino [67], Grasshopper [68], and simulation tools. The model

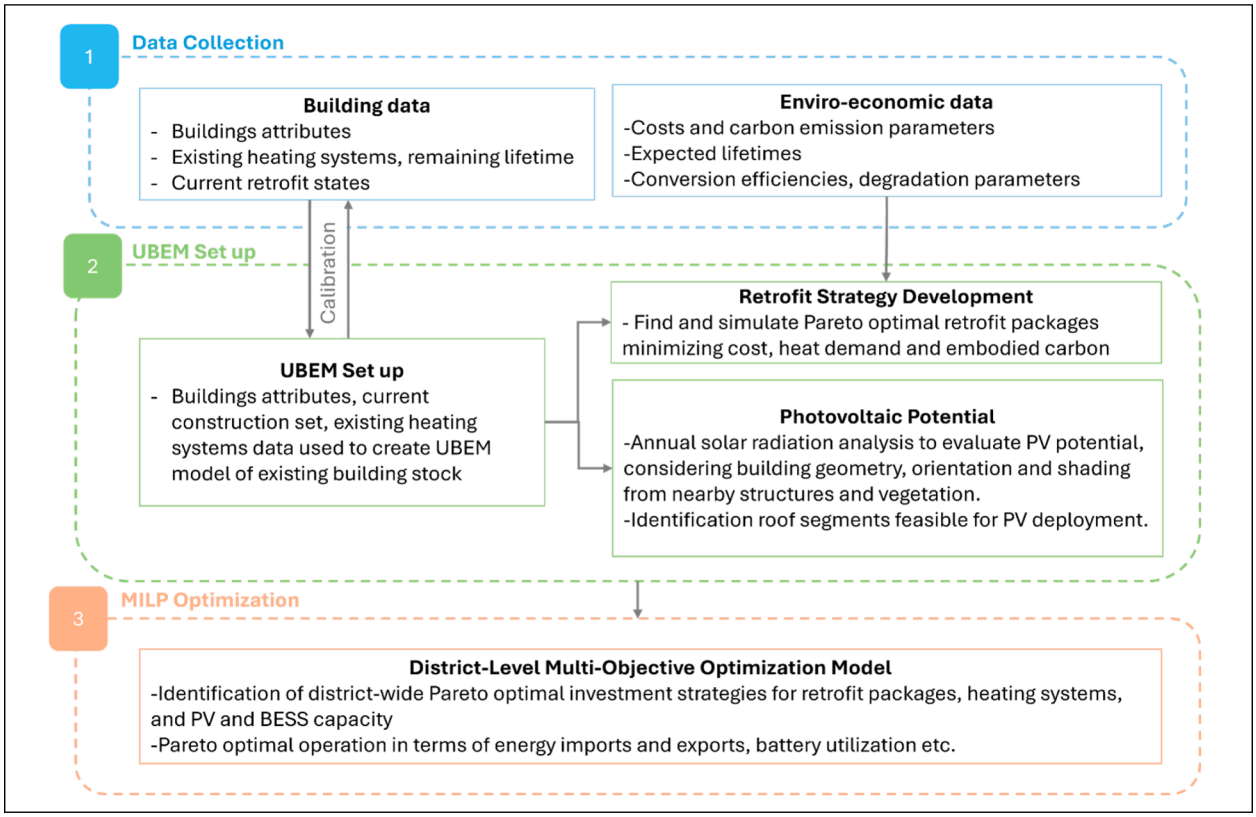

Fig. 1. Integrated UBEM–MILP framework for PED transformation.

replicates the neighbourhood's existing conditions and evaluated retrofit packages based on heating demand, material cost, and embodied carbon. The rooftop solar potential was assessed with PV production estimated via a PhotoVoltaic Geographical Information System (PVGIS) [69].

In the final step, outputs from the UBEM and solar analysis are integrated into a district-level MILP optimization model to identify cost- and carbon-efficient investment strategies over a 10-year horizon. The model selects retrofit packages, PV deployment, and heating systems while accounting for component degradation and shared infrastructure. It follows a bi-objective approach, minimizing the total system cost and both operational and embodied emissions, in line with PED goals.

3.1.1. *Step one: Data collection*

The implementation of the baseline energy model relies on the integration of a diverse set of spatial, geometric, and performance-related data. The main data sources used are from the Swedish mapping, cadastral and land registration authority (Lantmäteriet[70];), which were prioritized due to their authoritative and high-resolution geospatial data. Additional key sources include the national database Gripen with EPCs [71], U.S. Department Of Energy (DOE) commercial reference buildings [72], the local energy provider [21], and OneBuilding [73].

To support the bottom–up UBEM approach, data inputs were compiled for multiple building attributes, including geometry, building envelope characteristics, occupancy schedules, and energy demand. These datasets were essential for accurately replicating existing conditions, calibrating energy models, informing retrofit packages, and PV sizing strategies. Table 1 summarizes the primary data categories used in the UBEM, their sources and access conditions. 0

To support the analysis, a predefined material database was developed in collaboration with the property owners of the case district; see Tables A.6– A.8 in Appendix A for details. The database initially contained 38 candidate materials for cladding, insulation, and air/vapor barrier layers, selected based on market availability and technical feasibility. During stakeholder workshops, participants scored these materials by priority, reflecting both their current relevance and their curiosity to test emerging options, such as hemp-fiber insulation and recycled cotton insulation, to observe their performance within the modelling framework. Through this prioritization process, a subset of 18 materials was chosen for simulation. Based on these stakeholder preferences, retrofit packages were then formulated and integrated into the UBEM simulation model. The database includes key attributes for each material, such as embodied carbon emissions per unit ($kgCO_2e$), thermal conductivity (W/mK), average local market price (SEK), and available thicknesses and dimensions (mm). These values were used to calculate both the environmental and the economic impacts of the retrofit packages.

For the PV estimation, the annual electricity yield from rooftop PV systems, a crystalline silicon panel with a system efficiency of 14 % was assumed, based on PVGIS–SARAH3 database specifications [69]. The system was modelled with a nominal capacity of 1.0 kWp, and accounted for azimuth and tilt of existing buildings (see Table A.10), as well as shading effects from adjacent buildings and vegetation.

3.1.2. *Step two: UBEM set-up*

The second step focuses on setting up a UBEM replicating the neighbourhood's existing context through a 3D model and enabled simulation of various retrofit packages targeting three key performance indicators: heating demand, retrofit material cost, and embodied carbon emissions. The model was developed using Rhino and Grasshopper, integrated with Ladybug, Honeybee, Dragonfly, EnergyPlus, OpenStudio, and UrbanOpt. Rhino and Grasshopper were used for geometric modelling and parametric control, enabling seamless integration of spatial and building attribute data. Ladybug was used for solar analysis, while Honeybee and Dragonfly translated the geometry and metadata into simulation-ready inputs for EnergyPlus, which in turn served as the simulation engine

Table 1
Data sources and availability corresponding to the input parameters used in the UBEM and simulation tools.

Dataset	Description	Attribute	Source	Availability
Building footprint	2D GIS data representing the outline of buildings at ground level	Footprint geometry, spatial coordinates	Lantmäteriet	Open source
Building geometry and construction details	Architectural 2D building sections and floor plans	Building height, roof slope/ orientation, window–to–wall ratio, materials, occupancy program	Stadsbyggnadsförvaltningen	Access–on–request
Context buildings	Information on surrounding buildings for shading analysis and urban context modelling	Location, height, dimension	Lantmäteriet	Open source
Urban vegetation	Point cloud data and tree inventory for shading analysis	Location, height, diameter of trees	Lantmäteriet/DTCC Platform	Open source
Weather data	Typical Meteorological Year for Gothenburg	Hourly weather data	OneBuilding	Open source
Occupancy and internal loads	Standardized internal load schedules and profiles	Occupancy schedules, internal heat gains	DOE commercial reference buildings	Open source
Heating system and demand	Energy performance certificates and heating system info	Heating demand, system type	Boverket EPC database	Open source
Electricity demand	Hourly metered annual electricity consumption data	Building-level electricity demand	Local energy provider	Proprietary data

Table 2
Overview of UBEM: Simulation and analysis tools used in the study, including their operational scale, input and output data, and the design variables they influence within PED.

Tool	Simulation scale	Data input	Data output	PED affected design variable
EnergyPlus [50]	Building	Geometry, construction materials, HVAC systems, schedules, weather data	Heating/cooling demand, energy use, thermal comfort	Heating demand, retrofit impact
Ladybug plugin [52]	Building, district	Weather data, geometry, location	Solar radiation, sun path, daylighting metrics	Solar analysis
Honeybee plugin [52]	Building	Geometry, materials, schedules, HVAC templates, wea-ther data	Energy use, thermal loads, comformetrics	Building thermal performance
Dragonfly plugin [52]	District	Building geometry, site layout, weather, program definitions	Aggregated urban energy models, IDFs, and geometry for districts	District-scale energy modelling setup
OpenStudio [74]	District	High-level energy models (geometry, materials, systems, schedules), user-defined measures for retrofits or upgrades	Translated EnergyPlus model (in IDF format), calibration, scenario results	Testing different retrofit packages, energy model customization
UrbanOpt [53]	District	Building footprints, types, metadata (in Geojson file format), OpenStudio models, retrofit package configuration	District energy simulation, load profiles, PV potential, cost analysis	Energy balance, cost optimization, PV generation

for calculating heating demand and thermal loads, selected for its wide adoption, robust physics-based modelling capabilities, and compatibility with parametric workflows. OpenStudio facilitated the preparation and post-processing of EnergyPlus models and enabled integration with UrbanOpt, which was used to support district-scale energy simulations and scenario testing. Table 2 provides an overview of the UBEM and simulation tools used in the study.

Baseline energy model. As a starting point of the UBEM workflow, a baseline energy model was developed to reflect the existing conditions of buildings across the J̀attesten neighbourhood. The model aims to replicate the current state of the site using detailed 3D building geometries that incorporate building orientation and usage, as well ass shading effects from nearby structures and vegetation. To account for shading, the digital model incorporated vegetation—particularly trees—based on point cloud data from Lantmf́ateriet. Baseline simulations were run using a typical meteorological year weather file for Gothenburg, sourced from OneBuilding [73].

Air infiltration was set to a uniform rate of 0.00045 m^3/sm^2, derived from on-site blower door testing conducted on representative buildings. Since the DOE reference buildings are based on U.S. standards, modifications were made to reflect Swedish building practices and operational patterns. For example, for commercial premises such as small restaurants, and light-grocery shops matching the mixed-use activities observed on site, daily operating hours were set to 08:00–21:00, reflecting typical Swedish retail and food-service patterns. For educational facilities, separate schedules were developed for pre-schools and public schools to account for their distinct opening times, closing times, and internal gains, while public holidays and weekends were explicitly incorporated to capture periods of reduced or no occupancy. In addition, the heating system was modelled using a theoretical district heating system to estimate the heating energy required to condition the internal spaces, with temperature setpoint 21 °C aligned with the Swedish indoor climate regulations, and multi-family residential buildings included a common laundry room schedule—usually operated 08:00–22:00—with evening and weekend peaks typical of local user behavior.

The model was calibrated against 2023 heating demand data provided by Boverket, disaggregated by building use. The calibration accuracy was evaluated using the Mean Absolute Percentage Error (MAPE), which quantifies the average relative deviation between simulated and reference values. MAPE was selected for its intuitive percentage-based interpretation and suitability for comparing energy magnitudes across

buildings. Since the calibration targeted annual heating demand rather than hourly meter data, simulated hourly results were aggregated to annual totals before comparison. The calibration achieved a deviation below 5 %. Following calibration, a comprehensive UBEM was established to support retrofit packages simulations and district-level energy performance.

Annual solar radiation analysis was performed using Ladybug's incident radiation tools to calculate total solar exposure across all roof surfaces, accounting for azimuth, tilt, and dynamic shading conditions. The results were used to prioritize roof segments receiving the highest levels of incident radiation for further evaluation. To estimate the potential annual electricity generation, the selected roof areas were analysed using PVGIS, accessed programmatically to retrieve location-specific hourly and annual yield data. A system derate factor of 14 % was applied to account for inverter inefficiency, wiring, and temperature losses. Snow effects were implicitly considered through Typical Meteorological Year (TMY) weather data which provides representative hourly meteorological values over one year for a specific geographic location [75]. All studied buildings feature pitched roofs with angles of 15° or 30°, which by design minimize prolonged snow accumulation. Mounting constraints were not explicitly modelled, as the analysis focused on strategic planning—assessing the balance between local energy production and demand under planned roof renovations—rather than detailed installation design. This step enabled the estimation of on-site renewable energy production under standard system configurations.

Retrofit packages. Based on stakeholder consultations, the scope of retrofit packages in this study was limited to the building envelope—specifically roof and wall upgrades. The selected packages focused on exploring combinations of insulation, cladding, and air/vapor membrane materials. Full deep retrofit packages—such as window replacements, airtightness improvements, and mechanical system upgrades—were not included, in alignment with building owner preferences and feasibility constraints to evaluate only roof and wall specific interventions. This approach enables assessment of the marginal effects of these measures on heating demand, lifecycle cost, and embodied carbon. It facilitates analysis of the cost-benefit trade-offs of envelope improvements without the confounding influence of simultaneous HVAC or window retrofits. It also supports the identification of incremental renovation pathways, where envelope measures can be implemented first and subsequently complemented by additional upgrades if required. Such a targeted strategy provides clear evidence of the individual contribution of envelope retrofits, informing owners who favour phased investment strategies over immediate full deep renovation.

To operationalize the retrofit packages at scale, an automated parametric simulation workflow was developed, enabling the generation and evaluation of over 43 000 retrofit combinations for a representative residential building. The workflow assessed three main objectives:operational heating demand (kWh/m^{2}year), material embodied carbon (kgCO_2e), and retrofit material cost (SEK/m^2).

This significantly reduced input/output time and allowed rapid generation of thousands of simulations. Although the simulations were based on a residential building, the resulting packages were generalized to other building types in the district. Mixed-use buildings in Järnattesten share similar envelope characteristics with the residential typology. Thus, performance improvements were extrapolated using normalized baseline energy intensities, adjusted for each building category. This approach was adopted to maintain computational feasibility while ensuring representation of building stock diversity in the district-level MILP optimization. A multi-criteria filtering process—developed collaboratively with stakeholders—was used to identify the most relevant retrofit packages. Simulated configurations were ranked by *(1)* materials cost, *(2)* embodied carbon for building materials, *(3)* materials efficiency, and *(4)* practical feasibility, defined as technical constructability and market availability rather than current market uptake. During stakeholder workshops, participants reviewed and scored top-ranked packages, intentionally selecting a spectrum of solutions: cost-effective, average, and high-performance ecological options. This participatory approach was designed to demonstrate the study's primary aim of demonstrating the decision-support framework rather than to prescribe a single "optimal" retrofit from an energy or carbon perspective.

3.1.3. Step three: MILP optimization

In the final step, the outputs of the UBEM and solar analyses were integrated into a district-level MILP model. This optimization model identifies cost and carbon-efficient investment strategies over a ten-year planning horizon. Investment decisions—such as selecting retrofit packages, PV deployment, and heating system upgrades—are made at the start of the planning period and automatically renewed upon reaching the end of a component's technical lifetime. For a component that has not reached its technical lifetime at the end of the planning period, the monetary value is credited in terms of a salvage value (see (1), below), while its carbon emission footprint is proportionally scaled down—accounted for in (2), below. The model is single-stage since investment decisions are made once, i.e., at the start of the planning period. The model accounts for component degradation over time (e.g., PV or BESS capacity loss) and simulates operations at the individual building level, with shared infrastructure modelled through intra-district electricity transmission and a central BESS, with an hourly time resolution over the complete planning period. The MILP framework adopts a bi-objective optimization approach, minimizing *(i)* the total system cost and *(ii)* operational and embodied emissions, in alignment with the long-term goals of PED development.

Investments and operations are modelled using three types of variables: binary investment variables representing whether to install certain retrofit packages and technologies, continuous variables representing the capacity of the installed technologies, and continuous variables representing energy flows within the district. While binary investment variables and capacity variables are defined for each building and type of investment, the continuous variables for energy flows are defined for each building/BESS and time step.

The cost objective function is composed of investment costs, operating costs, and salvage values, primarily related to the buildings, denoted i. Investment costs are denoted z_{ip}^{ret} for retrofit packages p, and z_{is}^{tech} for technical systems s (including discounted costs for replacement of systems that are expected to meet their end of life during the planning period). The investment cost and discounted replacement costs of a district joint battery energy storage system is denoted z_{stor}. The operating cost, for each time step t, equals the difference between expenses for energy imports z_{it}^{imp} and income from energy exports z_{it}^{imp}. For investments that have not reached their technical life at the end of the planning horizon, salvage values—$z_{is}^{\text{tech,salv}}$ of technical system s, $z^{\text{stor,salv}}$ of the energy storage system, and $z_{ip}^{\text{ret,salv}}$ of retrofit package p—are credited back to the system. The cost objective is thus to minimize the sum of costs, expressed as

$$\sum_{i,p} \underbrace{z_{ip}^{\text{ret}}}_{\text{retrofit invest.}} + \sum_{i,s} \underbrace{z_{is}^{\text{tech}}}_{\text{technical invest.}} + \underbrace{z^{\text{stor}}}_{\text{storage invest.}} + \sum_{i,t} \underbrace{\left(z_{it}^{\text{imp}} - z_{it}^{\text{exp}}\right)}_{\text{operation}} - \sum_{i,s} \underbrace{z_{is}^{\text{tech,salv}}}_{\text{salvage}} - \underbrace{z^{\text{stor,salv}}}_{\text{salvage}} - \sum_{i,p} \underbrace{z_{ip}^{\text{ret,salv}}}_{\text{salvage}}, \tag{1}$$

which includes all system costs, although in practice these are shared between building owners and tenants. Technology investment costs are composed by a fixed and a capacity dependent cost; the same costs (although discounted) are assumed for replacements as for initial investments. Since data concerning the installed capacity of existing heating systems might not be available, we follow the example in [18] and let the model dimension the existing heating system "free of charge", while costs for replacement of an existing system with a retained capacity are accounted for.

The carbon emission objective function is composed of the embodied emissions for each building i from the selected retrofit packages p, denoted q_{ip}^{ret}, and from technical systems s (including replacements), denoted q_{is}^{tech}, of the embodied emissions from the district joint energy storage system, denoted q^{stor}, as well as of emissions from imported heat and electrical energy, denoted q_{it}^{imp}. The embodied emissions of technical systems and retrofits are defined as proportional to the share of their technical life they were in operation. The technical lives of retrofits are assumed to be 30 years. The embodied carbon emissions are considered on levels A1–A3 and B6, according to EN 15978; see [20]. Levels A4–A5, B2–B5, C1–C4, and D are excluded, due to lack of data availability, and uncertainty for transportation and post-demolition impact. The carbon emission objective is thus to minimize the sum of emissions, expressed as

$$\sum_{i,p} \underbrace{q_{ip}^{\text{ret}}}_{\text{retrofit emb. emiss.}} + \sum_{i,s} \underbrace{q_{is}^{\text{tech}}}_{\text{technical emb. emiss.}} + \underbrace{q^{\text{stor}}}_{\text{storage emb. emiss.}} + \sum_{i,t} \underbrace{q_{it}^{\text{imp}}}_{\text{oper. emiss.}} \tag{2}$$

The constraints of the model can be divided into two broad groups. The first group of constraints limits the installed capacity of technical systems, and restricts the capacity to zero for systems that are not invested in. These constraints connect binary investment variables and continuous capacity variables, and are relevant for building PV systems, building heating systems, and the district's BESS. The second group of constraints concerns energy balance and ensures that the energy demand for electricity and heating is met through import, storage, intra-district transmission, and PV production. Battery storage levels are controlled by battery dynamics constraints. For electricity storage and transmission, capacity degradation, maximum transmission capacity, and transmission losses are taken into account. Due to lack of data, we assume that there are no metering or tariff effects for the intra-district transmission.

The computational effort required to solve the problem is reduced by grouping residential buildings with regard to their normalized heat demand (kWh/m^2) in their current retrofit state. Buildings belonging to the same group are bound to be assigned the same retrofit package and heating system (see Fig. 7a), while PV investments are optimized for individual buildings. Other criteria for grouping, such as building age and geometry, did not provide useful groups, since all buildings in the district (except the school and preschool; see below) were built around the same time, with roughly the same building geometry. Building orientation and incident radiation are implicitly considered, as these influence the heat demand. A case study specific assumption is that no renovation will be done of the school buildings, since these buildings were built so recently that their renovation was considered economically infeasible be the stakeholders. Therefore, they each have only one retrofit package defined, representing their current state, while their PV and heating system investments as well as operation are still included in the optimization.

To solve the optimization problem with a planning horizon of ten years, a Benders decomposition approach [76] is utilized, by splitting the problem into a master problem—in which investments are determined—and one subproblem per year—in which optimal operations are determined given investment values computed by the master problem. Solutions to the subproblems are then utilized to update the master problem, and the master problem and the subproblems are alternately solved in a feedback loop. The years are decoupled by considering a yearly storage of energy in the battery instead of storage over the complete planning horizon, according to the approach developed in [57]. A weighted, normalized sum of the cost and emission objective functions is integrated with the Benders decomposition method to find Pareto optimal solutions. The model is implemented in Julia [77] with the JuMP package [78] for mathematical modelling and solved using the optimization solution software Gurobi [79]. The complete MILP model, decomposition and method development, implementation, extensive testing, and results are to be presented in a forthcoming article.

The retrofit packages identified using the UBEM model and the corresponding simulated yearly heating demands for each building are used as input data. The heating demand is assumed to be reduced by 2 % per year, to account for the effects of global warming. For electricity spot prices, we use historical data from 2022, characterized by high prices and volatility, and 2023, characterized by a mix of volatile and stable periods. The income from exporting electricity to the grid is calculated as the spot price minus 0.05 SEK/kWh. The district heating system is assumed to become carbon neutral within four years from the start of the planning horizon, based on information from the local DHS provider [21]. The same cost data is used in each year, increased yearly by 2 %, the target inflation rate in Sweden [80]. Technical parameters for materials and technical systems (heating systems, PV systems, and battery) are provided by academic sources and industry; see Tables A.6–A.9 in Appendix A for details.

3.2. Case study: Järnattesten, Gothenburg

Järnattesten is a mixed-use neighbourhood in Gothenburg, Sweden, comprising 22 residential buildings together consisting of approximately 500 housing units, two mixed-use buildings, one school, and one preschool (see Fig. 2a). The buildings in the studied neighbourhood represent typical buildings in Sweden. Hence, there is a high replication potential for the results to be implemented and upscaled in other Swedish districts. The residential and mixed-use buildings were constructed in the late 1950s, and the school was built in 1957, representing the older building stock that may require an extensive retrofitting to enhance the energy performance and efficiency. Each residential building consists of a basement and three floors, characteristic of mid-20th-century low-rise lamellar apartment building structures with plastered facades and balconies. In contrast, the preschool (built in 2018) represents more modern constructions with a timber facade following higher energy performance standards. Building owners express a need for renovation to align with the City of Gothenburg's environmental and decarbonization goals. The buildings on site are connected to the DHS network as the primary heating system. The buildings feature pitched roofs with slopes in the interval 15–40°, introducing a variability in their suitability for PV systems. Roof areas differ between buildings, and the orientation of each surface plays a key role in PV investment decisions and electricity production.

This study examines energy efficiency improvements through retrofit strategies targeting roof and wall assemblies, with the objective of reducing heating demand, enhancing building envelope performance. In parallel, the analysis also evaluates the integration of RES, with particular emphasis on assessing the solar potential of building roofs for PV installations. Future PV deployment is guided by simulated solar radiation data, prioritizing roof segments based on their orientation and solar exposure. The aim is to assess whether local renewable energy production can offset or exceed baseline electricity demand. The baseline electricity demand includes both household electricity consumption and the operational energy of the property owner, such as lighting and appliances in shared spaces (e.g., stairwells, public laundries, and circulation areas).

4. Results

4.1. Neighbourhood characterization and baseline modelling

Based on high-resolution geometric modelling (see Fig. 2b), a baseline energy model was developed for the Järnattesten neighbourhood. The baseline model was calibrated using EPC heating demand data for each building type. The baseline model was calibrated using existing heating demand data for each building type. The calibration process ensured that the simulated results aligned closely with observed data, achieving

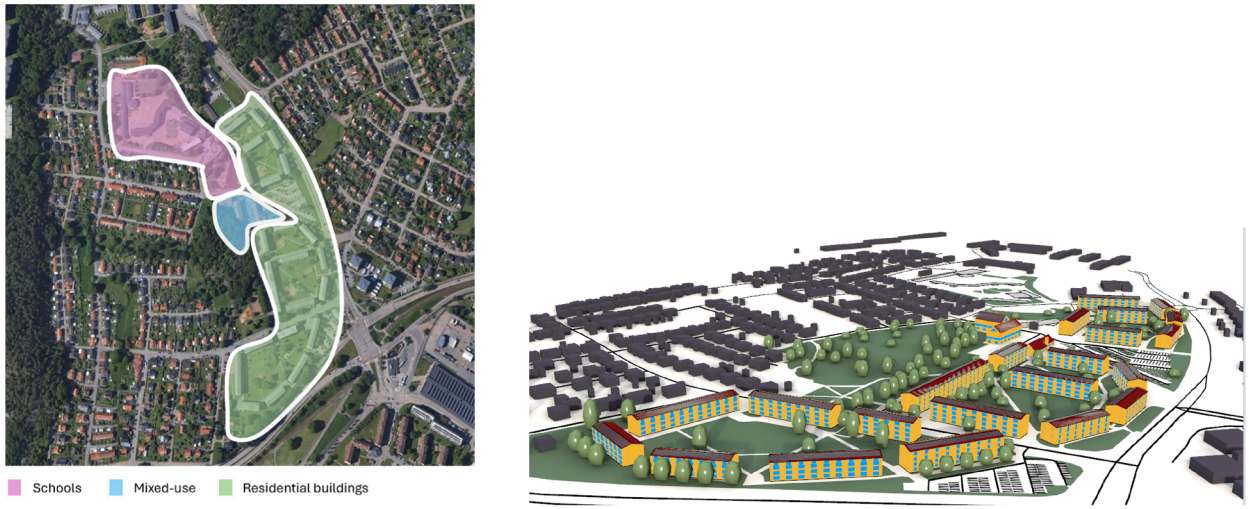

(a) Site map highlighting different land uses. **(b)** 3D model setup including context and surrounding areas.

Fig. 2. Site map and 3D model of the J̈attesten neighborhood in Gothenburg, Sweden.

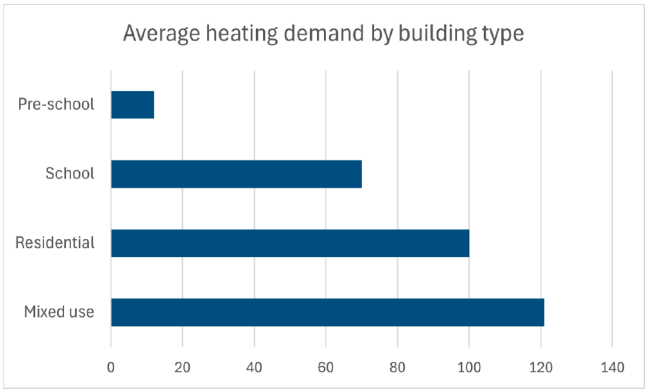

Fig. 3. Average heating demand (kWh/m^2) by building type.

an error margin below 5 %. Simulated annual heating demand varied significantly across the district, influenced by construction type, orientation, and internal zoning. Among the building categories, mixed-use buildings exhibited the highest average heating demand, at 120 kWh/m^2 a year (see Fig. 3). This was followed by school buildings at 108 kWh/m^2 a year, residential buildings at 100 kWh/m^2 a year, and finally preschool buildings, which showed the lowest demand at 89 kWh/m^2 a year.

For PV installation, roof segments with limited solar exposure—primarily those with unfavourable orientations or extensive shading receiving the least solar irradiance—were excluded from further consideration. The priority was given south-, southwest-, and west-facing segments with the highest annual solar gains. Under these conditions, the estimated annual yield was 864.94 kWh per installed kilowatt-peak, with total system losses—including temperature effects, angle of incidence, and spectral losses—amounting to 22.59 %. These values served as the benchmark for evaluating solar potential across all buildings in the study area. These baseline models highlight the potential for energy performance improvements through building envelope retrofit and integration of rooftop PV systems to produce electricity locally, and to assess the potential of transforming J̈attesten into a PED.

4.2. Buildings performance simulation and retrofit packages

From the over 43 000 parametric simulations conducted (see Fig. 4), the retrofit packages targeting heating demand reduction—representing a medium-depth intervention—resulted in significant performance gains. Across residential buildings, average normalized heating demand decreased from 100 to 84.02 kWh/m^{2}year, representing a 15.98 % reduction. For mixed-use buildings, the same packages yielded a greater reduction due to higher baseline demand: from 120 to 53.24 kWh/m^{2}year, corresponding to a 55.63 % decrease. These results reflect the amplified benefits of envelope improvements in high-demand buildings.

In practice, retrofit decisions often require balancing energy performance improvements with financial and environmental constraints. To capture this complexity, two Pareto front analyses were conducted to visualize the trade-offs between the three key performance indicators: heating demand, material embodied carbon, and material cost. Fig. 5(a) shows the relation between cost and embodied carbon, with color indicating heating demand, while Fig. 5(b) displays the trade-off between heating demand and embodied carbon, with cost as the color gradient. These plots illustrate the wide spectrum of potential retrofit configurations and highlight the diversity of optimal paths depending on the selected priority—whether cost-efficiency, carbon reduction, or energy savings.

From the full simulation set, six retrofit packages (RPs) were selected for integration into the district-level MILP optimization model (see Table 3). Limiting the number of RPs helped maintaining a feasible computing time, which increases exponentially with the number of binary variables in the MILP model [81].

The present UBEM framework extends beyond a static baseline by incorporating Future Climate Scenarios (FCSs) to evaluate how today's renovation decisions may influence indoor thermal comfort, overheating risk, and future cooling demand under projected temperature increases. Four shared socioeconomic pathways scenarios with escalating levels of warming were used to assess the long-term performance of retrofit and PV strategies, ensuring that measures designed for present conditions remain effective in maintaining acceptable indoor temperatures and mitigating overheating as the climate changes; detailed results are presented in [27].

4.3. Solar potential

Fig. 7(b) presents the modelled nominal PV yield (in kWh/kWp) for each building based on its geometry and solar exposure (see Fig. 7a). Roof segments receiving less than 750 kWh/kWp annually were classified as low-performing and excluded from further analysis. Segments with annual yields in the interval 750–900 kWh/kWp were categorized as medium-performing, while those exceeding 900 kWh/kWp annually

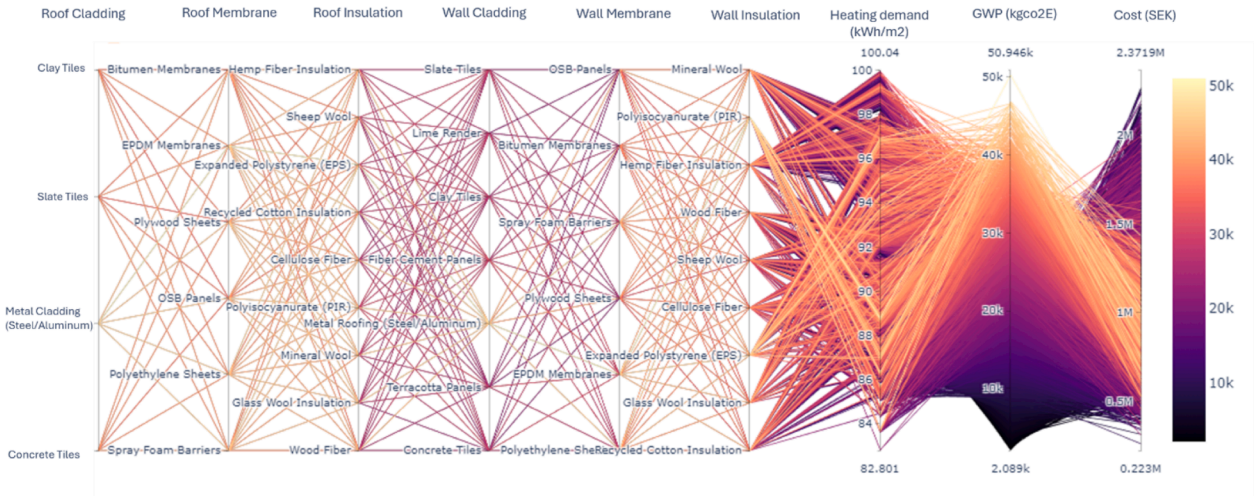

Fig. 4. Parallel coordinates plot visualizing the results of over 43 000 parametric simulations of roof and wall retrofit packages combinations run on representative residential building. Each line represents a unique material configuration and is linked to simulated performance outcomes in terms of heating demand (kWh/m^{2}year), material embodied carbon (kgCO$_2$e), and retrofit material cost (SEK).

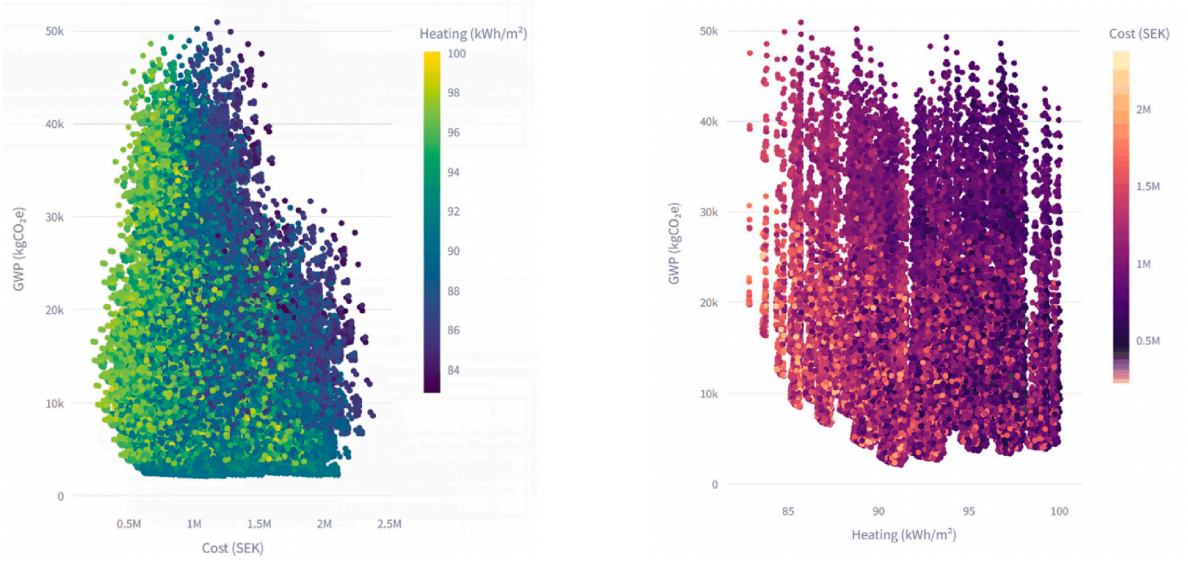

(a) Trade-off between cost (SEK) and embodied carbon (kgCO$_2$e), colour indicating heating demand (in kWh/m^{2}year).

(b) Trade-off between heating demand (kWh/m^{2}year) and embodied carbon (kgCO$_2$e), colour indicating cost (SEK).

Fig. 5. Pareto front visualizations of simulated retrofit packages across three performance indicators: operational heating demand, embodied carbon (Global Warming Potential, GWP), and retrofit cost. The plots highlight the diversity of retrofit outcomes and support the identification of optimal packages based on different stakeholder priorities.

were considered high-performing and prioritized for PV installation. The spatial distribution of yields reflects the influence of shading from surrounding structures and vegetation, as well as roof orientation and tilt—the latter is disclosed in Table A.10. This mapping process supported the identification of high-priority buildings for decentralized renewable energy generation within the PED strategy. The medium- and high-performing roof segments made up the feasible PV investments in the MILP optimization model described in Section 3.1.3. The total PV capacity installed across residential and mixed-use rooftops was estimated at 2641.18 kWp, a substantial renewable energy integration considering the roof pitch and shading constraints. Based on annual solar radiation modelling and system performance estimates, PV systems could supply approximately 60 % of the total electricity demand across the site. This result underlines the critical role of passive building features, such as roof orientation and shading conditions, in realizing PED ambitions. The decision to prioritize south-, southwest-, and west-facing roofs ensured that installed PV arrays operate close to their technical potential. Nevertheless, the remaining 40 % dependency on external electricity supply points to the need for complementary strategies, such as demand side management, energy storage, or additional Building Integrated Photo-Voltaic (BIPV) solutions.

4.4. District-level bi-objective optimization

The UBEM can exist as a standalone system and provide feasible investment configurations, although with no quality guarantee, while the MILP engine requires a backhaul UBEM. The advantage of the MILP engine is the possibility to explore the set of solutions that are guaranteed to be Pareto optimal, i.e., no investment configuration can possess both a lower cost and lower emissions than those of any Pareto optimal configuration.

Table 3
Overview of the six retrofit packages (RP) selected from the Pareto analysis for inclusion in the district-level MILP optimization model.

RP ID	Objective	Average heating demand reduction (%)	Carbon emission ($kgCO_2e/m^2$)	Materials cost (SEK/m^2)	Wall materials	Roof materials
1	lowest CO_2	7.45	0.97	509.56	Lime render, plywood sheets, & sheep wool	Concrete tiles, plywood sheets, & sheep wool
2	lowest CO_2	7.44	0.97	496.38	Lime render, plywood sheets, & sheep wool	Concrete tiles, OSB panels, & sheep wool
3	heat reduction	15.98	9.39	1062.97	Terracotta panels, spray foam barrier, & PIR	Clay tiles, spray foam barrier, & PIR
4	heat reduction	15.97	10.34	862.13	Fiber cement panels, spray foam barrier, & PIR	Clay tiles, spray foam barrier, & PIR
5	lowest cost	1.78	64.60	110.92	Lime render, polyethylene sheets, & EPS	Concrete tiles, polyethylene sheets, & EPS
6	lowest cost	1.60	6.71	116.17	Lime render, polyethylene sheets, & EPS	Concrete tiles, polyethylene sheets, & glass wool

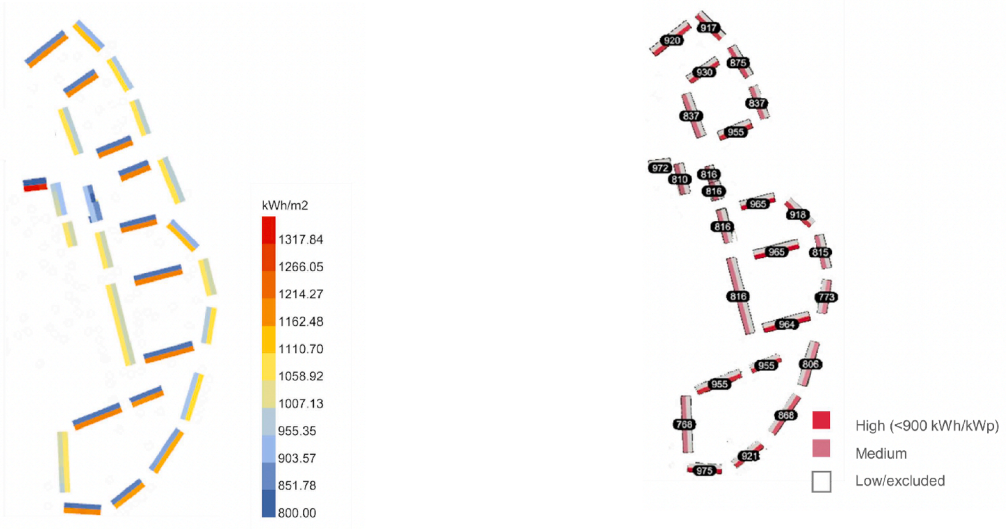

(a) Incident annual solar radiation (in kWh/m^2 a year) across all roof surfaces based on the Ladybug analysis.

(b) Nominal PV yield (in kWh/kWp a year) per roof segment, calculated using PVGIS under standard configuration assumptions. The roof segments are classified into high- (>900), medium- (750–900), and low-performing (<750), guiding the selection for feasible PV deployment in the MILP optimization model.

Fig. 6. Solar performance mapping of rooftops in the Jättesten neighbourhood.

The MILP requires a significant amount of input data, including technical and economical parameters, heat demand data for each building and retrofit package, as well as solar irradiance and electricity demand data, all with an hourly resolution. The connection to UBEM is therefore necessary for running the optimization model. The quality and reliability of the optimized solutions also depends on a high accuracy of the simulated input data. The normalized heating demand for each residential building and the resulting grouping of buildings in the optimization model are depicted in Fig. 7(a).

Two scenarios with different spot price profiles were tested: Setup 2023, with more stable spot prices, and Setup 2022, with volatile spot prices.

The computed Pareto optimal solutions to the bi-objective MILP optimization model using Setup 2023 (lower left, green dots, 1–9) and Setup 2022 (upper right, magenta dots, 10–22) are shown in Fig. 7(b). The markers + (green) and • (magenta) represent the 'as is' solution for Setup 2023 and 2022, respectively; for these solutions, no new investments are made, while operation is optimized; hence, they serve as reference points for evaluating the benefits of further interventions. Note that cost outcome for the 'as is' solution differ between the two setups due to the variation in spot price profiles. For each setup, the end points of the curve are computed by minimizing CO_2 emissions and total cost, respectively. The points are numbered from left to right, with the minimum emission solution numbered 1 (Setup 2022) and 10 (Setup 2023), and the minimum cost solution numbered 9 and 22, respectively.

Details of the corresponding investment decisions for the Pareto optimal solutions are provided in Table 4 (Setup 2023) and Table 5 (Setup 2022), and include BESS capacity, PV area utilization (as percentage of available area), and grid dependency ratio—defined as the average proportion of electricity demand met through grid imports over the full planning horizon. The selected retrofit package and heating system are specified for each residential building group and solution, the retrofit number indicating the selected retrofit package 0–6, with 0 corresponding to "no retrofit".

4.4.1. Results and analysis of the a scenario with more stable spot prices: Setup 2023

Setup 2023 shows a clear trend to select Air Source Heat Pump (ASHP) as heating system and to retrofitting residential buildings when approaching the cost optimal solution. The retrofit investment

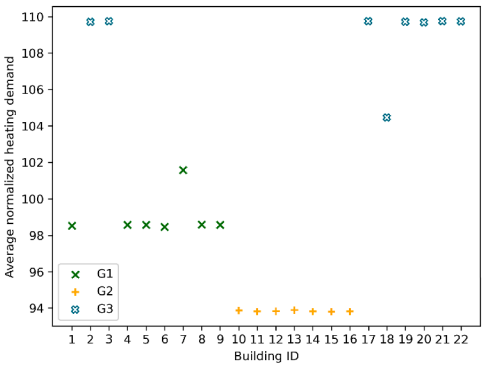

(a) Grouping of *residential buildings* with respect to normalized heat demand. The different markers indicate the groups, G1, G2, and G3, of residential buildings employed in the optimization model as well as in the presentation of the results. All buildings within a group should be assigned the same type of heating system and the same type of retrofit package. This grouping of residential buildings was used for both Setup 2023 and Setup 2022.

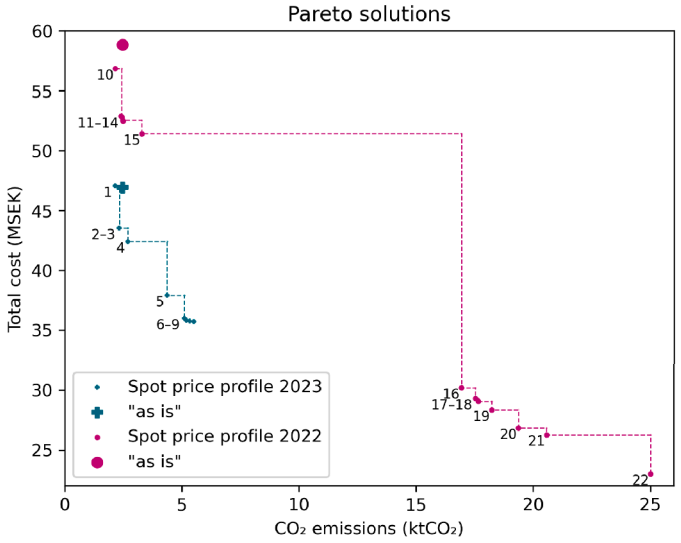

(b) Computed points on the Pareto front of the emissions and cost minimization objectives, as well as the 'as is' solution, for Setup 2023 (lower left, green; Pareto points 1–9) and Setup 2022 (upper right, magenta; Pareto points 10–22). See Tables 4–5 for solution details.

Fig. 7. Grouping of residential buildings and computed points on the Pareto front.

Table 4
Optimal investments for each computed Pareto optimal solution of Setup 2023; see Fig. 7(b). The columns G1–G3 (denoting the three groups of residential buildings; see Fig. 7a) and Mixed-use contain the index of the selected retrofit package (#) and the selected heating system (∘ DHS; • ASHP). The columns School and Preschool contain the selected heating system (∘ DHS; • ASHP).

Pareto point (#)	Cost (MSEK)	Emissions ($ktCO_2e$)	G1	G2	G3	Mixed-use	School	Preschool	Grid dep. **ratio**	PV (%)	BESS capacity (kWh)
			(package #)			(heating system)	(heating system)				
'as is'	46.93	2.47	0 ∘	0 ∘	0 ∘	0 ∘	∘	∘	100	0	0
1	47.05	2.15	0 ∘	0 ∘	0 ∘	0 ∘	∘	∘	86	100	0
2	43.54	2.33	6 ∘	6 ∘	6 ∘	0 ∘	∘	∘	86	100	0
3	43.53	2.33	6 ∘	6 ∘	6 ∘	0 ∘	∘	∘	86	100	0
4	42.39	2.69	6 ∘	6 ∘	6 ∘	0 ∘	•	∘	86	100	0
5	37.91	4.36	6 •	6 ∘	6 •	0 ∘	•	∘	88	100	0
6	35.97	5.10	6 •	6 •	6 •	0 ∘	•	∘	88	100	0
7	35.83	5.19	6 •	6 •	6 •	0 •	•	•	93	100	0
8	35.75	5.33	6 •	6 •	6 •	0 •	•	•	96	56	0
9	35.72	5.51	6 •	6 •	6 •	0 •	•	•	100	0	0

configuration to select package 6 (one of the lowest cost alternatives; see Table 3) for all three groups of residential buildings is identical in all Pareto optimal solutions, except the emission optimal solution with notably no retrofit investment for any building.

The sole difference in investments between the emissions optimal solution (Pareto point 1) and Pareto point 2 is the retrofitting of residential buildings done in the latter. This retrofit investment reduces the district-wide heating demand by 14 % and lowers costs by 7.5 % but increases the emissions by 8 % (see Table 4). This suggests that the embodied emissions from the investments are not offset by the resulting reduction in heat demand—likely due to the close–to carbon neutral supply of DHS. In contrast, the monetary investments are recovered over the planning period. The large distance between Pareto points 4 and 5 can be explained by differences in heating system investments. Starting from Pareto point 2 and moving rightward along the frontier, investments shift from DHS to ASHP for all groups of buildings, while other investments remain unchanged, implying that the choice of heating system is the main driver of both cost and emissions.

PV systems are utilized in all Pareto optimal solutions, except the cost-optimal point (Pareto point 9), which suggests that PV can reduce emissions at a relatively low cost. This can be found by comparing solutions near the cost-optimal point: The solution of point 8 differs from that of point 9 only in its PV investment, which results in 5.8 % lower CO_2 emissions and 0.3 % higher costs. Similarly, the only difference between the 'as is' solution and the emissions optimal solution (point 1) is again the inclusion of PV, resulting in a reduction of carbon emissions by 13 % at a cost increase of 0.26 %.

The lowest grid dependency achieved is 86 %, when 100 % of the available roof area is utilized for PV. As the selected heating systems shift to ASHP the grid dependency increases due to an increased electricity demand: from 86 % in Pareto points 1 and 2—where all buildings have DHS and 100 % PV—to 93 % in Pareto point 8—where all buildings have ASHP and PV utilization of 56 %. The cost optimal solution has a 100 % grid dependency ratio.

The Pareto optimal solutions corresponding to points 2–9 possess an export of electricity, which occurs when the produced electricity exceeds the district's total demand, and the spot price for selling electricity is positive. The amount of exported electricity is the larger for solutions in which most buildings keep DHS, and decreases as investments shift to ASHP, due to an increased self-consumption.

Table 5
Optimal investments for each computed Pareto optimal solution of Setup 2022; see Fig. 7(b). The columns G1–G3 (denoting the three groups of residential buildings; see Fig. 7a) and Mixed-use contain the index of the selected retrofit package (#) and the selected heating system (∘ DHS; • ASHP; ▲ GSHP). The columns School and Preschool contain the selected heating system (∘ DHS; • ASHP; ▲ GSHP).

Pareto point (#)	Cost (MSEK)	Emissions ($ktCO_2e$)	G1 (package #)	G2 (package #)	G3 (package #)	Mixed-use (package # heating system)	School (heating system)	Preschool (heating system)	Grid dep. ratio	PV (%)	BESS capacity (kWh)
'as is'	58.86	2.47	0 ∘	0 ∘	0 ∘	0 ∘	∘	∘	100	0	0
10	56.87	2.15	0 ∘	0 ∘	0 ∘	0 ∘	∘	∘	86	100	0
11	52.88	2.40	6 ∘	6 ∘	6 ∘	0 ∘	∘	∘	79	100	427
12	52.83	2.44	6 ∘	6 ∘	6 ∘	0 ∘	∘	∘	75	100	841
13	52.54	2.47	6 ∘	6 ∘	6 ∘	0 ∘	∘	∘	74	100	761
14	52.49	2.48	6 ∘	6 ∘	6 ∘	0 ∘	∘	∘	73	100	844
15	51.40	3.05	6 ∘	6 ∘	6 ∘	6 •	∘	∘	67	100	2092
16	30.19	16.93	6 ∘	6 ∘	6 ∘	1 ▲	∘	∘	63	100	26,988
17	29.30	17.53	6 ∘	6 ∘	6 ∘	0 ∘	∘	▲	64	100	26,988
18	29.06	17.65	6 ∘	6 ∘	6 ∘	0 ∘	∘	▲	64	100	26,988
19	28.33	18.22	6 ∘	6 ∘	6 ∘	0 ∘	∘	▲	65	100	26,988
20	26.83	19.37	6 ∘	6 ∘	6 ∘	0 ∘	∘	∘	68	100	26,988
21	26.27	20.58	6 ∘	6 ∘	6 ∘	0 ∘	∘	∘	77	100	26,988
22	25.01	23.00	6 •	6 ∘	6 ∘	0 ∘	∘	∘	64	100	26,988

4.4.2. Results for and analysis of the scenario with volatile spot prices: Setup 2022

The solutions for Setup 2022 reveal a strikingly different investment pattern as compared to Setup 2023, favoring investments that reduce the impact of spot price fluctuation on total costs (DHS as opposed to ASHP), and systems that can exploit and offer resilience against volatile electricity prices (investments in BESS and PV).

As reported in Table 5, the heating systems largely remain DHS across the Pareto points, with a few exceptions where Ground Source Heat Pump (GSHP) is selected for the mixed-use building (Pareto point 16) and the preschool (Pareto points 17–19). ASHP is selected for the mixed-use building in Pareto point 15. An investment in ASHP is also present in the cost optimal solution, for group G1 of residential buildings. This investment is combined with the largest possible investment in PV as well as in BESS, exploiting the daily fluctuation in spot prices.

The PV utilization is 100 % in all Pareto optimal solutions, including the cost optimal one (point 22). Further, there is a BESS investment in each solution except the emission optimal solution (point 10) and solutions near the cost optimal solution possess the largest possible BESS capacity investment. This indicates that BESS investments contribute significantly to total emissions by a large amount of embodied CO_2 emissions, while simultaneously offering a potential to reduce the total system costs, through an effective charging policy. Both export and import of electricity is considerably larger in Setup 2022 as compared to Setup 2023, indicating a capitalization on volatile spot prices. Additionally, the solutions with large BESS investments achieve the lowest grid dependency ratios, of ∼64 %.

Similar to Setup 2023, the only difference between the 'as is' solution and the emissions optimal investment is the PV utilization, resulting in a 13 % emissions reduction and a 3.4 % cost reduction. The emissions optimal solution is thus both cheaper and less carbon intense than the 'as is' solution; the corresponding investments are identical to those of Setup 2023, which is expected since the carbon emission data are the same. Further, the retrofit investment trend across the Pareto optimal solutions is the same as for Setup 2023: package 6 (one of the lowest cost alternatives; see Table 3) is selected for all residential buildings in all Pareto optimal solutions, except the emissions optimal solution.

4.5. Solution analysis and PED compliance evaluation

This section evaluates the Järnattesten neighbourhood's potential to achieve core PED tenets—i.e., net-zero annual energy imports, net-zero carbon emissions, and local renewable energy surplus—by synthesizing the bi-objective optimization outcomes (Section 4.4) for the two electricity spot price scenarios—Setup 2023 (stable prices) and Setup 2022 (volatile prices)—against the 'as is' solution for the respective scenarios.

4.5.1. Energy balance and self-sufficiency

A primary PED goal is to minimize reliance on external energy. While an initial UBEM analysis suggested that rooftop PV could meet ∼60 % of Järnattesten's electricity demand, the MILP optimization reveals a more nuanced path to self-sufficiency. Under stable prices (Setup 2023), the 100 % utilization of PV in the carbon optimal solution still results in 86 % grid dependency over ten years, with BESS investments not being optimal. Conversely, under volatile prices (Setup 2022), the cost optimal solution combines 100 % PV with maximum BESS capacity, reducing grid dependency to 64 %; the most favorable dependency achieved is ∼63 % with extensive PV and BESS. These findings highlight that while rooftop PV and BESS integration substantially improves self-sufficiency (particularly in Setup 2022), achieving net-zero annual electricity imports solely with the evaluated rooftop PV and retrofit measures is a considerable challenge. A significant import requirement persists, suggesting the need for further interventions like BIPV or other local RES.

4.5.2. Carbon emission reduction

Considering both embodied and operational emissions, the baseline 'as is' solution incurs 2.47 $ktCO_2e$ over ten years. The carbon optimal strategy in both price setups (maximizing PV, retaining the existing, soon–to–be carbon neutral DHS, and notably, avoiding retrofit embodied carbon) reduces emissions by ∼13 % to 2.15 $ktCO_2e$. Some Pareto optimal solutions with shallow, low-cost retrofits combined with PV also achieve lower lifecycle costs and emissions than the 'as is' case. Strategies prioritizing cost under volatile prices (Setup 2022)—especially those heavily investing in BESS—can, however, lead to substantially higher emissions (e.g., 23.00 $ktCO_2e$ for the cost optimal solution). Net-zero carbon emissions, encompassing all lifecycle aspects, were not achieved in any Pareto optimal solution. The embodied carbon from retrofits proves challenging to offset against an already low-carbon DHS, an effect magnified by the assumed future carbon neutrality of the DHS. Additional optimization results showed the same investment configurations in the cost and emissions optimal solution, also when the assumption of a decarbonized DHS was removed, i.e., the emissions being at today's level over the complete planning period.

4.5.3. Surplus renewable energy generation

Achieving a net annual energy surplus—a defining PED aspiration—appears unlikely for Järnattesten with the evaluated interventions. Although maximized rooftop PV meets up to 60 % of electricity needs,

optimized solutions still show considerable grid dependency (63–86 %). While electricity export to the grid occurs in many solutions (often facilitated by BESS and price arbitrage), a net positive annual energy balance was not realized. Reaching an energy surplus would require substantially augmented RES capacity beyond the scope of this study.

4.5.4. Overall PED compliance

The Järnattesten case study demonstrates that achieving full PED status (net-zero energy import, net-zero carbon, energy surplus) with the considered envelope retrofits, rooftop PV, and BESS capacities is a challenge for an existing neighborhood.

- *Net-Zero Carbon:* Demonstrable progress is made, with optimized solutions reducing emissions significantly compared to the baseline, heavily relying on PV and DHS decarbonization.
- *Reducing Energy Imports:* Grid dependency can be markedly reduced (from 100 % to as low as 63 % with PV and BESS).
- *Energy Surplus:* This remains out of reach without additional RES.

The PED transformation inherently involves critical trade-offs between initial investment costs, embodied carbon of retrofits and systems, operational carbon savings, and resilience to energy price volatility. Sweden's low-carbon energy context means that the carbon optimal solution is sensitive to embodied carbon, sometimes forgoing energetic retrofits. Furthermore, electricity price volatility significantly influences optimal investment strategies, incentivizing PV and BESS investments for cost containment and energy arbitrage, which can enhance grid independence but sometimes at the cost of higher overall emissions. Further progress towards comprehensive PED compliance would require supplementary RES, carefully selected deeper retrofits balancing embodied and operational carbon, and integration with broader urban systems.

5. Discussion

This study employs an integrated UBEM and MILP framework to explore pathways for transforming the existing Järnattesten neighbourhood in Gothenburg, Sweden, into a PED. The results reveal complex trade-offs and highlight critical factors influencing the feasibility and optimal strategies for achieving PED targets.

5.1. Interpreting the path to PED compliance in an existing swedish neighbourhood

A central finding is that achieving full PED status—encompassing net-zero annual energy imports, net-zero carbon emissions, and a renewable energy surplus—presents substantial challenges for an existing neighbourhood like Järnattesten, even with extensive interventions, in the form of investments in building renovations, new heating systems, and renewable energy production. While significant progress can be made, particularly towards carbon reduction, the aspiration of energy surplus with rooftop PV as the primary local renewable source appears largely unattainable. The simulations indicate that rooftop PV could meet roughly 60 % of electricity demand. However, even in optimal solution with 100 % PV deployment, grid dependency remained high (at 63–86 %), influenced by the price profile scenario (Setup 2023 or Setup 2022) and inclusion of BESS. This underscores a potential need to re-evaluate PED definitions for existing urban contexts or to explore a wider array of local renewable energy generation and storage technologies beyond building-integrated solutions if strict energy surplus targets are to be met.

The Swedish energy context, characterized by a low-carbon electricity grid and the prevalence of efficient DHS with high renewable shares, profoundly shapes the optimization outcomes. The 'as is' solution (no new investments are made), with its reliance on existing DHS, demonstrated total emissions (2.47 $ktCO_2e$) remarkably close to the value of the carbon optimal solution (2.15 $ktCO_2e$). This suggests that in regions with already decarbonized energy supplies, the marginal operational carbon benefits of deep energy retrofits can be diminished, bringing the embodied carbon of retrofit materials and energy system components to the forefront of decision-making. Indeed, the carbon optimal solutions in both setups paradoxically involved no building envelope retrofits, thereby avoiding embodied carbon, and instead prioritized maximizing PV generation and retaining the DHS (assumed to become operationally carbon neutral). This finding contrasts with contexts where fossil fuel-based heating dominates, in which case deep retrofits typically yield more substantial operational carbon savings that can more readily offset their embodied carbon.

5.2. The role of economic conditions and technological choices

The influence of electricity spot price volatility on optimal investment strategies is a key observation. Under the more stable price conditions (Setup 2023), BESS did not feature in Pareto optimal solutions. Conversely, the highly volatile prices in Setup 2022 rendered BESS investments economically attractive, significantly reducing grid dependency (to 63 %) and enabling cost savings through energy arbitrage. In this volatile setup, PV utilization was consistently maximized across all Pareto optimal solutions, including the cost-optimal one, and DHS was more frequently retained, likely due to its predictable cost structure compared to electricity-driven heating systems exposed to price peaks. This highlights that the business case for BESS and the optimal heating system configuration is highly sensitive to local electricity market dynamics and tariff structures. For PED development, this implies that flexibility measures like BESS may be crucial not only for grid services but also for economic resilience in markets with fluctuating prices.

Shallow retrofit packages (e.g., package 6, lowest cost) emerged as economically viable and offered a good compromise, reducing heating demand (e.g., by 14 % district-wide in Pareto point 2, Setup 2023) and achieving lower lifecycle costs and emissions than the 'as is' solution in several instances. The decision to pursue deeper retrofits would require careful consideration of material choices to minimize embodied carbon or a longer-term perspective where energy prices might shift more dramatically, or where non-energy benefits (e.g., comfort, property value) are more heavily weighted.

5.3. Synergies and trade-offs in system configuration

The interplay between PV generation, heating system choice, and retrofit level was evident. Maximizing PV generation was a consistent strategy for emission reduction across all Pareto optimal solutions. However, the increased electricity demand from electrifying heating (e.g., shifting from DHS to ASHP) could increase grid dependency if not adequately met by on-site generation and storage, as seen in the rise from 86 % to 93 % grid dependency when shifting to ASHP in Setup 2023 (Table 4, Pareto points 2 and 7). The choice of heating system was a primary driver of both cost and emissions in many Pareto optimal solutions. While DHS offered a low-carbon baseline (especially with its future decarbonization assumption), ASHPs provided a pathway to lower operational costs in some Pareto optimal solutions, albeit with higher electricity consumption and potentially higher emissions if the grid's carbon intensity does not decrease as rapidly as that of the DHS.

The results affirm the necessity of the integrated UBEM–MILP approach. The detailed building performance data from UBEM provided essential inputs for the MILP, allowing for a nuanced evaluation of retrofit packages. The MILP, in turn, could explore a vast solution space of technology combinations and operational strategies that would be intractable with simulation alone, thereby identifying Pareto optimal solutions that reveal the critical trade-offs between economic and environmental objectives.

5.4. Implications for policy and practice

For policymakers and urban planners in Sweden and similar contexts, this study suggests that PED strategies should be carefully tailored. Promoting maximal deployment of on-site renewables like PV is clearly beneficial. However, incentive structures for building retrofits should consider the embodied carbon of building materials and construction elements accounting for the actual operational carbon savings achievable given the local energy supply mix. A blanket approach favoring very deep retrofits might not always be the most carbon-efficient strategy if it incurs high embodied emissions that are not offset by operational savings from an already clean heating source. Financial support mechanisms for BESS could be particularly effective in regions with volatile electricity prices or where grid flexibility is highly valued. Furthermore, the significant role of DHS decarbonization highlights the importance of continued investment in and greening of district energy networks as a cornerstone of urban energy transitions that is still affordable for tenants and residents. Building owners, in turn, are presented with evidence that even shallow, cost-effective retrofits combined with PV can yield tangible benefits, while decisions on heating system replacement require careful consideration of long-term energy price trends and carbon implications.

The findings of this study contribute to the understanding of PED implementation in existing urban areas, particularly highlighting the influence of local energy systems and economic conditions. While the specific numerical results are context-dependent, the identified trade-offs and the demonstrated utility of an integrated modelling and optimization approach offer valuable insights for researchers, policymakers, and practitioners working towards sustainable urban energy futures.

5.5. Limitations

A key challenge in this process was the lack of data on the cost, dimensions, embodied carbon, and thermal conductivity of recycled metal panels and timber for external cladding, due to the scarcity of information on reused materials within the Swedish context. Further research outside of Sweden, along with direct inquiries to local retailers in the reuse and recycling sectors, could provide insights into the cost and dimensions of these materials. While circularity is recognized as an important aspect of PED transitions, end-of-life scenarios, reuse, and recycling were not explicitly modelled in this study because of scope and data constraints.

While the DOE commercial reference buildings provide a standardized framework for modelling occupancy schedules, they are based on building usage patterns typical of the United States. These include assumptions about operational hours, internal load densities, and occupant behavior that may not align with Swedish practices, which differ in terms of work hours, seasonal occupancy variation, and energy use behavior. To address this limitation, the default DOE occupancy schedules were modified in this study to reflect Swedish operational hours and use patterns more accurately, as described in the methodology section on UBEM setup (Section 3.1.2).

The present study focuses on demonstrating an integrated UBEM-MILP framework for evaluating retrofit and PV strategies for PED. While the UBEM extends beyond a static baseline by incorporating FCSs to assess how today's renovation decisions may influence indoor thermal comfort, overheating risk, and future cooling demand under projected temperature increases, detailed results of this analysis are reported separately in [27] and are hence not presented here.

For the optimization tool, there is a limitation in data availability and predictability of future spot market electricity costs, district heating costs, as well as the embodied carbon emissions of these energy carriers. While two different scenarios for the spot price profiles were evaluated, the DHS costs were assumed to be constant. For embodied carbon emissions, the assumption was made that the DHS would become carbon neutral during the planning period, but removing this assumption did not change the carbon optimal solution. The development of embodied carbon emissions of grid electricity was not considered. Future work could therefore include testing alternative development trajectories for these parameters, providing a more comprehensive sensitivity analysis beyond the cost sensitivity presented here.

The exclusion of the school and preschool from retrofit investments and heating system investments was a case study specific assumption, that makes our solutions pessimistic bounds on the actual cost and carbon optimal solutions, meaning that the objective value optimization problem without this exclusion might be lower than the one attained by us, and the emissions of the emission optimal solution might be lower one attained by us.

Grouping of residential buildings for heating system and retrofit investments was done to achieve feasible computation times, but was also assumed to be in line with building owners' preference to reduce the number of unique renovation investments within a district. Due to this restriction, the solutions are pessimistic bounds on the optimal solutions of the unrestricted problem (without grouping of residential buildings).

Finally, socio-economic consequences of deep renovation measures for tenants and residents have been outside the scope of this study but earlier studies showed that these effects can be significant for this stakeholder group [30,32–34] and need to be acknowled in a sustainable transition pathway.

5.6. Future studies

Building on this research, future studies could explore several key avenues to further enhance the understanding and implementation of Positive Energy Districts in existing urban neighbourhoods. Expanding the portfolio of RES beyond rooftop PV, to include ambitious BIPV strategies and other locally available RES technologies, is crucial for approaching true energy surplus goals. Further investigation into comprehensive retrofit strategies should more deeply address the challenge of embodied carbon, for instance by prioritizing innovative low-carbon materials, systematically evaluating the potential of reused and recycled building components and fully integrating circular economy principles into the lifecycle assessment. Future modelling efforts could also yield more holistic insights by integrating PED transformation pathways with other critical urban systems, such as sustainable transportation networks and waste-to-energy solutions. Moreover, enhancing the optimization framework by incorporating stochastic methods to manage uncertainties related to future energy prices, technological advancements, and occupant behaviour would improve the robustness of long-term planning. Finally, given the complexities of implementation, dedicated research into adaptive governance models, novel financing mechanisms, and effective stakeholder engagement strategies will be vital for overcoming the practical barriers to transforming existing urban districts into successful PEDs.

6. Conclusion

This study developed and applied an integrated Urban Building Energy Modelling (UBEM) and Mixed-Integer Linear Programming (MILP) framework to optimize Positive Energy District (PED) transformation pathways in an existing Swedish neighbourhood. The methodology co-optimized building retrofits, PhotoVoltaic (PV) system, and Battery Energy Storage System (BESS) capacities to minimize lifecycle costs and carbon emissions (including embodied carbon) over a 10-year horizon.

The J[3]attesten case study demonstrated that achieving full PED status—encompassing net-zero energy imports, net-zero total carbon emissions, and an energy surplus—is highly challenging with the considered interventions (envelope retrofits, rooftop PV, and BESS). While significant progress was shown, with optimized solutions reducing grid dependency from 100 % to as low as ~63 % (with PV and BESS under volatile prices) and overall carbon emissions by ~13 %

compared to the baseline, the goals of net-zero energy import and complete carbon neutrality (including embodied aspects) were not met. An energy surplus also proved unattainable with the evaluated measures.

The findings underscore crucial trade-offs between initial investment costs, embodied carbon of materials and systems, operational carbon savings, and energy system resilience to volatile electricity prices. Optimal investment strategies were found to be highly sensitive to the specific local energy context, such as Sweden's low-carbon electricity grid and the anticipated decarbonization of district heating, as well as to economic conditions like electricity price fluctuations, which particularly influence the viability and impact of BESS. The primary contribution of this research is a replicable decision-support methodology offering useful insights and identifying promising strategies for PED planning, enabling stakeholders to navigate the complex techno-economic and environmental trade-offs inherent in transforming existing urban areas. By the use of a mathematical decomposition method, investments and operations can be jointly optimized over a 10-year planning horizon with hourly resolution, avoiding reliance on typical-day representations. This integrated framework provides valuable insights for policymakers, urban planners, and stakeholders in developing effective strategies for the sustainable energy transition of established neighborhoods. Future work should explore broader RES integration and circular economy approaches to further advance PED objectives.

CRediT authorship contribution statement

Sara Abouebeid: Writing – review editing, Writing – original draft, Visualization, Validation, Methodology, Formal analysis, Data curation; **Jenny Enerbäck:** Writing – review editing, Writing – original draft, Project administration, Methodology, Conceptualization; **Elena Malakhatka:** Writing – review editing, Writing – original draft, Supervision,Project administration, Methodology, Conceptualization; **Ann-Brith Strömberg:** Writing – review editing, Supervision, Methodology; **David Sindelar:** Writing – original draft, Data curation; **Mohammadreza Mazidi:** Data curation; **Araavind Sridha:** Data curation; **Holger Wallbaum:** Writing – review editing, Supervision, Conceptualization; **Liane Thuvander:** Writing – review editing, Supervision, Project administration, Funding acquisition, Conceptualization.

7. Data availability statement

Data supporting the findings of this study are available from the corresponding author upon request. The electricity data are private and cannot be shared publicly. The EPC dataset used for model calibration contains proprietary information from the Swedish National Board of Housing, Building and Planning, and is available from the authors upon request. The decision support tool developed during this study is available from the corresponding author upon request.

Data availability

Data will be made available on request.

Declaration of competing interests

Liane Thuvander reports financial support was provided by Swedish Energy Agency. If there are other authors, they declare that they have no known competing financial interests or personal relationships that could have appeared to influence the work reported in this paper.

Acknowledgments

The computations were enabled by resources provided by the National Academic Infrastructure for Supercomputing in Sweden (NAISS), partially funded by the Swedish Research Council through grant agreement no. 2022-06725. This study is part of the DT4PED project which has received funding within the Joint Programming Initiative Urban Europe, financially supported by the Swedish Energy Agency (P2022-01028), the Fonden af 20. December, Solar A/S, Solar Sverige AB, and the Energy Area of Advance at Chalmers University of Technology; it is also connected the Digital Twin Cities Centre, supported by Sweden's Innovation Agency Vinnova Grant No. 2019-00041. We thank all partners of the DT4PED project, specifically the housing company Poseidon, F̀orvaltnings AB Framtiden, and Stadsfastighetsf̀orvaltningen for their support, and the local energy provider G̀oteborg Energi for providing data. The author(s) used ChatGPT (OpenAI) only for language editing, grammar and clarity improvements. All conceptual development, methodological formulation, analyses and interpretation were solely developed by the authors.

Appendix A. Materials, technological, and economical data

Table A.6
External cladding material parameters.

External cladding	Application	Environmental impact A1–A5 ($kgCO_2e$)	Average initial product price (SEK)	λ-value (W/mK)	Dimension (mm)
Fiber Cement Panels	walls	84.51429	1127.95	0.3	$8 \times 1192 \times 2500$
Terracotta Panels	walls	0.73612	46.89	0.6	$19 \times 185 \times 380$
Lime Render	6.4	85.81	0.9		
Clay Tiles	roofs	0.90342	31	0.6	$30 \times 266 \times 420$
Slate Tiles	roofs	0.991413	37	0.29	$7 \times 500 \times 300$
Metal Roofing (Steel/Aluminium)	roofs	86.027439	438.375	50	$0 \times 1050 \times 2500$
Concrete Tiles	roofs	1.09212	10.41	1.7	330×420
Green Roofs	roofs	0.885	1336.27	0.29	$90 \times 1000 \times 1000$

Table A.7
Air and vapor membrane materials parameters.

Air & vapor membrane	Application	Environmental impact A1–A5 ($kgCO_2e$)	Average initial product price (SEK)	λ-value (W/mK)	Dimension (mm)
Polyethylene Sheets	walls, roofs	40.0231	499	0.16	$0 \times 2700 \times 2500$
Bitumen Membranes	walls, roofs	25.8158	917	0.22	$3 \times 1000 \times 7000$
EPDM Membranes	walls, roofs	74.2	1386	0.29	$4 \times 1400 \times 10000$
OSB Panels	walls, roofs	10.63165	268	0.13	$11 \times 1197 \times 2500$
Plywood Sheets	walls, roofs	9.47936	399	0.14	$12 \times 1200 \times 2500$
Spray Foam Barriers	walls, roofs	26.6	257.5	0.036	$80 \times 1000 \times 1000$

Table A.8
Insulation materials parameters.

Insulation material	Application	Environmental impact A1–A5 ($kgCO_2e$)	Average initial product price (SEK)	λ-value (W/mK)	Dimension (mm)
Glass Wool Insulation	walls, roofs	10.61325	24.86	0.035	$45 \times 560 \times 1160$
Hemp Fiber Insulation	walls, roofs	2.06997	80.75	0.04	$40 \times 1100 \times 600$
Cellulose Fiber	walls, roofs	7.02195	73.22	0.036	$95 \times 565 \times 1170$
Wood Fiber	walls, roofs	4.73552	84.44	0.038	$95 \times 565 \times 1220$
Sheep Wool	walls, roofs	2.97	1058.4	0.0425	$100 \times 600 \times 6000$
Mineral Wool	walls, roofs	1.56066	74.8	0.033	$45 \times 565 \times 1170$
Recycled Cotton Insulation	walls, roofs	7.767	94	0.039	$100 \times 600 \times 1200$
Expanded Polystyrene (EPS)	walls, roofs	24.864768	60.4	0.036	$50 \times 1200 \times 2400$
Polyisocyanurate (PIR)	walls, roofs	23.28	739.5	0.022	$100 \times 600 \times 2400$

Table A.9
Input parameter data used in the MILP optimization model, with corresponding data sources, countries, and reference years.

Category	Description	Value	Unit	Source	
PV	Lifetime of PV system	27.5	Years	[82]	SE 2025
	Area dependent cost of installing PV technology	2932.2	SEK/m^2	[83]	SE 2025
	Area dependent cost of PV technology	2400	SEK/m^2	[82]	SE 2025
	Area dependent embodied carbon emission factor	121.56	$kgCO_2/m^2$	[84]	SE 2024
	Area dependent cost of work on roof	792	SEK/m^2	[82]	SE 2024
	PV conversion efficiency	20	%	[85]	US 2025
Battery	Lifetime of BESS	10	Years	[82]	SE 2025
	Capacity dependent cost of BESS, including installation	3500	SEK/kWh	[82]	SE 2025
	Capacity dependent embodied carbon emission factor	45	$kgCO_2$/kWh	[86]	SE 2023
	Charging and discharging efficiency	96	%	[18]	CH 2022
	Maximum charging and discharging rates	25	%	[18]	CH 2022
Heating	Lifetime of GSHP system	20	Years	[19]	CH 2017
	Lifetime of ASHP system	20	Years	[19]	CH 2017
	Lifetime of electric heating system	30	Years	[19]	CH 2017
	Capacity dependent embodied carbon emissions of GSHP system	273	$kgCO_2$/kW	[18]	CH 2022
	Capacity dependent embodied carbon emissions of ASHP system	364	$kgCO_2$/kW	[18]	CH 2022
	Capacity dependent embodied carbon emissions of electric heating system	75	$kgCO_2$/kW	[87]	SE 2025
	Fixed cost of installing GSHP system	262 500	SEK	[88]	SE 2025
	Fixed cost of installing ASHP system	30 000	SEK	[88]	SE 2025
	Fixed cost of installing electric heating system	130 670	SEK	[19]	CH 2017
	Conversion efficiency for heating in GSHP system	400	%	[19]	CH 2017
	Conversion efficiency for heating in ASHP system	300	%	[19]	CH 2017
	Conversion efficiency for heating in electric heating system	100	%	[19]	CH 2017
	Cost of district heating (DHS; energy import) during time step t (winter)	0.91	SEK/kWh	[21]	SE 2025
	Cost of district heating (DHS; energy import) during time step t (summer)	0.4186	SEK/kWh	[21]	SE 2025
Electricity	Cost of electricity imported from the grid at time step t	0.6	SEK/kWh	[89]	SE 2023
	Carbon emission factor of imported electricity at time step t	0.157	$kgCO_2$/kWh	[21]	SE 2024
Investments	Interest rate on investments	3.3	%	[90]	SE 2025

Table A.10
Usable roof areas, azimuths, and roof tilt angles. Buildings #1–22 have just two roof segments; hence data for roofs #3 and #4 are not applicable.

Building	Roof #1		Roof #2		Roof #3		Roof #4		Tilt of roofs #1–4
(#)	Azimuth (°)	Area (m^2)	Azimuth (°)	Area (m^2)	Azimuth (°)	Area (m^2)	Azimuth (°)	Area (m^2)	(°)
1	75	447	−104	447	–	–	–	–	15
2	70	262	−109	262	–	–	–	–	15
3	157	198	−22	198	–	–	–	–	15
4	165	198	−14	198	–	–	–	–	15
5	44	198	−135	198	–	–	–	–	15
6	75	198	−104	198	–	–	–	–	15
7	164	268	−15	265	–	–	–	–	15
8	98	198	−81	198	–	–	–	–	15
9	75	198	−104	198	–	–	–	–	15
10	158	182	−21	182	–	–	–	–	15
11	107	261	−72	261	–	–	–	–	15
12	123	261	−56	261	–	–	–	–	15
13	3	198	−176	198	–	–	–	–	15
14	87	326	−92	326	–	–	–	–	15
15	158	271	−21	271	–	–	–	–	15
16	141	197	−38	197	–	–	–	–	15
17	145	262	−34	262	–	–	–	–	15
18	165	261	−14	261	–	–	–	–	15
19	45	198	−134	198	–	–	–	–	15
20	145	196	−34	196	–	–	–	–	15
21	59	199	−120	199	–	–	–	–	15
22	70	198	−109	198	–	–	–	–	15
23	75	111	−104	151	75	151	−104	151	30
24	173	185	−6	185	77	238	−102	238	30

References

[1] IEA, Energy Technology Perspectives 2016, Technical Report ISBN 978-92-64-25234-9, International Energy Agency, Paris, 2016. accessed: 2025-04-12, https://www.iea.org/reports/energy-technology-perspectives-2016.

[2] I. Aparisi-Cerdá, D. Ribó-Pérez, T. Gómez-Navarro, M. García-Melón, J. Peris-Blanes, Prioritising positive energy districts to achieve carbon neutral cities: Delphi-DANP approach, Renew. Sustain. Energy Rev. 203 (2024) 114764. https://doi.org/10.1016/j.rser.2024.114764

[3] W.K. Fong, M. Sotos, M. Doust, S. Schultz, global protocol for community-scale greenhouse gas emission inventories (GPC), 2014, . accessed: 2025-09-12, https://ghgprotocol.org/greenhouse-gas-protocol-accounting-reporting-standard-cities.

[4] W. Wu, H.M. Skye, Residential net-zero energy buildings: review and perspective, Renew. Sustain. Energy Rev. 142 (2021) 110859. https://doi.org/10.1016/j.rser.2021.110859

[5] S. Koutra, V. Becue, M.-A. Gallas, C.S. Ioakimidis, Towards the development of a net-zero energy district evaluation approach: a review of sustainable approaches and assessment tools, Sustain. Cit. Soc. 39 (2018) 784–800. https://doi.org/10.1016/j.scs.2018.03.011

[6] A. Blumberga, R. Vanaga, R. Freimanis, D. Blumberga, J. Antužs, A. Krastiš, I. Jankovskis, E. Bondars, S. Treija, Transition from traditional historic urban block to positive energy block, Energy 202 (2020) 117485. https://doi.org/10.1016/j.energy.2020.117485

[7] F. Guarino, R. Rincione, C. Mateu, M. Teixidó, L.F. Cabeza, M. Cellura, Renovation assessment of building districts: case studies and implications to the positive energy districts definition, Energy Build. 296 (2023) 113414. https://doi.org/10.1016/j.enbuild.2023.113414

[8] JPI Urban Europe, Positive Energy Districts (PED), 2021, accessed: 2025-09-12, https://jpi-urbaneurope.eu/ped/.

[9] M. Cellura, A. Fichera, F. Guarino, R. Volpe, Sustainable development goals and performance measurement of positive energy district: a methodological approach, in: Sustainability in Energy and Buildings 2021, 263, Springer Nature Singapore, 2022, pp. 519–527. https://doi.org/{10.1007/978-981-16-6269-00_43}

[10] A. Buonomano, F. Guarino, The impact of thermophysical properties and hysteresis effects on the energy performance simulation of PCM wallboards: experimental studies, modelling, and validation, Renew. Sustain. Energy Rev. 126 (2020) 109807. https://doi.org/10.1016/j.rser.2020.109807

[11] I. Marotta, F. Guarino, M. Cellura, S. Longo, Investigation of design strategies and quantification of energy flexibility in buildings: a case-study in Southern Italy, J. Build. Eng. 41 (2021) 102392. https://doi.org/10.1016/j.jobe.2021.102392

[12] C. Citadini De Oliveira, I. Catão Martins Vaz, E. Ghisi, Retrofit strategies to improve energy efficiency in buildings: an integrative review, Energy Build. 321 (2024) 114624. https://doi.org/10.1016/j.enbuild.2024.114624

[13] E. Ball, H. Haberstock, U. Lynar, A. Akrzipczyk, Holistic Strategies for Energy Efficient Refurbishment of the Housing Stock and Renewal of the Energy Supply System, 2011, accessed: 2025-09-12, https://digital.zlb.de/viewer/metadata/15707740/.

[14] D.-I. Stanica, A. Karasu, D. Brandt, M. Kriegel, S. Brandt, C. Steffan, A methodology to support the decision-making process for energy retrofitting at district scale, Energy Build. 238 (2021) 110842. https://doi.org/10.1016/j.enbuild.2021.110842

[15] M. Thebault, L. Gaillard, Optimization of the integration of photovoltaic systems on buildings for self-consumption–case study in France, City Env. Interac. 10 (2021) 100057. https://doi.org/10.1016/j.cacint.2021.100057

[16] C. Granfeldt, A.-B. Strömberg, L. Göransson, A Lagrangian relaxation approach to an electricity system investment model with a high temporal resolution, OR Spectrum 45 (4) (2023) 1263–1294. https://doi.org/10.1007/s00291-023-00736-w

[17] G. Mavromatidis, I. Petkov, MANGO: a novel optimization model for the long-term, multi-stage planning of decentralized multi-energy systems, Appl. Energy 288 (2021) 116585. https://doi.org/10.1016/j.apenergy.2021.116585

[18] I. Petkov, G. Mavromatidis, C. Knoeri, J. Allan, V.H. Hoffmann, MANGOret: an optimization framework for the long-term investment planning of building multi-energy system and envelope retrofits, Appl. Energy 314 (2022) 118901. https://doi.org/10.1016/j.apenergy.2022.118901

[19] R. Wu, G. Mavromatidis, K. Orehounig, J. Carmeliet, Multiobjective optimisation of energy systems and building envelope retrofit in a residential community, Appl. Energy 190 (2017) 634–649. https://doi.org/10.1016/j.apenergy.2016.12.161

[20] CEN, Sustainability of construction works—Assessment of environmental performance of buildings—Calculation method, 2011, accessed: 22-09-2025, https://standards.iteh.ai/catalog/standards/cen/62c22cef-5666-4719-91f9-c21cb6aa0ab3/en-15978-2011?srsltid=AfmBOopJ16evFwplA57C3qq624qLJ5qIvX6NpIrXibujkuU7KcV2L38e.

[21] Göteborg Energi, Gothenburg Energy, 2024, accessed: 2025-09-12, https://www.goteborgenergi.se/english/.

[22] S. Institute, Energy use in Sweden, 2024, accessed: 23-09-2025, https://sweden.se/climate/sustainability/energy-use-in-sweden.

[23] Mangold, Mikael, Making the housing stock more energy efficient, 2024, accessed: 2025-09-12, https://www.ri.se/en/making-the-housing-stock-more-energy-efficient.

[24] S. Erba, L. Pagliano, Combining sufficiency, efficiency and flexibility to achieve positive energy districts targets, Energies 14 (15) (2021) 4697. https://doi.org/10.3390/en14154697

[25] S. D'Oca, A. Ferrante, C. Ferrer, R. Pernetti, A. Gralka, R. Sebastian, P. Op 't Veld, Technical, financial, and social barriers and challenges in deep building renovation: integration of lessons learned from the H2020 cluster projects, Buildings 8 (12) (2018) 174. https://doi.org/10.3390/buildings8120174

[26] C. Langston, Green adaptive reuse: issues and strategies for the built environment, in: D.D. Wu (Ed.), Modeling Risk Management in Sustainable Construction, Springer Berlin, 2011, pp. 199–209. https://doi.org/{10.1007/978-3-642-15243-6_23}

[27] S. Abouebeid, E. Malakhatha, H. Wallbaum, L. Thuvander, Future-proofing positive energy districts: Climate change impacts on energy demand and supply in Jättesten, Gothenburg, 2025. presdented at the CISBAT International Scientific Conference.

[28] H. Egerlid, X. Wang, L. Thuvander, D. Maiullari, Carbon efficiency of passive cooling measures in future climate scenarios: renovating multi-family residential buildings in a Swedish context, Energy Build. 334 (2025). https://doi.org/10.1016/j.enbuild.2025.115502

[29] K. Riahi, Representative Concentration Pathways Database (RCP), 2009, acccessed: 23-09-2025, https://iiasa.ac.at/models-tools-data/rcp.

[30] S.N. Ma'bdeh, Y.A. Gani, L. Obeidat, M. Aloshan, Affordability assessment of passive retrofitting measures for residential buildings using life cycle assessment, Heliyon 9 (2023). https://doi.org/10.1016/j.heliyon.2023.e13574

[31] B. Risholt, B. Time, A.G. Hestnes, Sustainability assessment of nearly zero energy renovation of dwellings based on energy, economy and home quality indicators, Energy Build. 60 (2013) 217–224. https://doi.org/10.1016/j.enbuild.2012.12.017

[32] B. Ástmarsson, P. Anker Jensen, E. Maslesa, Sustainable renovation of residential buildings and the landlord/tenant dilemma, Energy Policy 63 (2013) 355–362. https://doi.org/10.1016/j.enpol.2013.08.046

[33] H. Lind, Pricing principles and incentives for energy efficiency investments in multi-family rental housing: the case of Sweden, Energy Policy 49 (2012) 528–530. https://doi.org/10.1016/j.enpol.2012.06.054

[34] M. Mangold, M. Österbring, H. Wallbaum, L. Thuvander, P. Femenias, Socio-economic impact of renovation and energy retrofitting of the Gothenburg building stock, Energy Build. 123 (2016). https://doi.org/10.1016/j.enbuild.2016.04.033

[35] M. Formolli, G. Lobaccaro, J. Kanters, Solar energy in the nordic built environment: challenges, opportunities and barriers, Energies 14 (24) (2021) 8410. https://doi.org/10.3390/en14248410

[36] S.R. Penaka, K. Feng, T. Olofsson, A. Rebbling, W. Lu, Improved energy retrofit decision making through enhanced bottom-up building stock modelling, Energy Build. 318 (2024) 114492. https://doi.org/10.1016/j.enbuild.2024.114492

[37] O. Koral Iseri, A. Duran, I. Canlı, C. Meral Akgul, S. Kalkan, I. Gursel Dino, A method for zone-level urban building energy modeling in data-scarce built environments, Energy Build. 337 (2025) 115620. https://doi.org/10.1016/j.enbuild.2025.115620

[38] L.G. Swan, V.I. Ugursal, Modeling of end-use energy consumption in the residential sector: a review of modeling techniques, Renew. Sustain. Energy Rev. 13 (8) (2009) 1819–1835. https://doi.org/10.1016/j.rser.2008.09.033

[39] M. Österbring, C. Camarasa, C. Nägeli, L. Thuvander, H. Wallbaum, Prioritizing deep renovation for housing portfolios, Energy Build. 202 (2019) 109361. https://doi.org/10.1016/j.enbuild.2019.109361

[40] M. Ferrando, F. Causone, T. Hong, Y. Chen, Urban building energy modeling (UBEM) tools: a state-of-the-art review of bottom-up physics-based approaches, Sustain. Cit. Soc. 62 (2020) 102408. https://doi.org/10.1016/j.scs.2020.102408

[41] N. Buckley, G. Mills, C. Reinhart, Z.M. Berzolla, Using urban building energy modelling (UBEM) to support the new European union's green deal: case study of Dublin Ireland, Energy Build. 247 (2021) 111115. https://doi.org/10.1016/j.enbuild.2021.111115

[42] Y. Ma, W. Deng, J. Xie, T. Heath, Y. Xiang, Y. Hong, Generating prototypical residential building geometry models using a new hybrid approach, Build. Simul. 15 (1) (2022) 17–28. https://doi.org/10.1007/s12273-021-0779-6

[43] C. Nägeli, L. Thuvander, H. Wallbaum, R. Cachia, S. Stortecky, A. Hainoun, Methodologies for synthetic spatial building stock modelling: data-availability-adapted approaches for the spatial analysis of building stock energy demand, Energies 15 (18) (2022) 6738. https://doi.org/10.3390/en15186738

[44] A.L. Pisello, J.E. Taylor, X. Xu, F. Cotana, Inter-building effect: simulating the impact of a network of buildings on the accuracy of building energy performance predictions, Build. Environ. 58 (2012) 37–45. https://doi.org/10.1016/j.buildenv.2012.06.017

[45] A. Dimoudi, M. Nikolopoulou, Vegetation in the urban environment: microclimatic analysis and benefits, Energy Build. 35 (1) (2003) 69–76. https://doi.org/10.1016/S0378-7788(02)00081-6

[46] X. Xu, H. AzariJafari, J. Gregory, L. Norford, R. Kirchain, An integrated model for quantifying the impacts of pavement albedo and urban morphology on building energy demand, Energy Build. 211 (2020) 109759. https://doi.org/10.1016/j.enbuild.2020.109759

[47] C.F. Reinhart, C. Cerezo Davila, Urban building energy modeling—A review of a nascent field, Build. Environ. 97 (2016) 196–202. https://doi.org/10.1016/j.buildenv.2015.12.001

[48] L.E. Excell, A. Nutkiewicz, R.K. Jain, Multi-scale retrofit pathways for improving building performance and energy equity across cities: a UBEM framework, Energy Build. 324 (2024) 114931. https://doi.org/10.1016/j.enbuild.2024.114931

[49] A. Nutkiewicz, B. Choi, R.K. Jain, Exploring the influence of urban context on building energy retrofit performance: a hybrid simulation and data-driven approach, Adv. Appl. Energy 3 (2021) 100038. https://doi.org/10.1016/j.adapen.2021.100038

[50] Y.Q. Ang, Z.M. Berzolla, C.F. Reinhart, From concept to application: a review of use cases in urban building energy modeling, Appl. Energy 279 (2020) 115738. https://doi.org/10.1016/j.apenergy.2020.115738

[51] Z. Deng, Y. Chen, J. Yang, F. Causone, AutoBPS: a tool for urban building energy modeling to support energy efficiency improvement at city-scale, Energy Build. 282 (2023) 112794. https://doi.org/10.1016/j.enbuild.2023.112794

[52] M. Sadeghipour Roudsari, C. Mackey, Ladybug tools [Computer software], 2012, accessed: 22-09-2025, https://www.ladybug.tools/.

[53] A.f. S.E. LLC, URBANopt [Computer software], 2019, accessed: 22-09-2025.

[54] T. Charan, C. Mackey, A. Irani, B. Polly, S. Ray, K. Fleming, R. El Kontar, N. Moore, T. Elgindy, D. Cutler, M.S. Roudsari, D. Goldwasser, Integration of open-source URBANopt and dragonfly energy modeling capabilities into practitioner

workflows for district-scale planning and design, Energies 14 (18) (2021) 5931. https://doi.org/10.3390/en14185931
[55] D. Kong, A. Cheshmehzangi, Z. Zhiang, S. Pourroostaei Ardakani, T. Gu, Urban building energy modeling (UBEM): a systematic review of challenges and opportunities, Energy Effic. 16 (2023). https://doi.org/10.1007/s12053-023-10147-z
[56] C. Wang, S. Wei, S. Du, D. Zhuang, Y. Li, X. Shi, X. Jin, X. Zhou, A systematic method to develop three dimensional geometry models of buildings for urban building energy modeling, Sustain. Cit. Soc. 71 (2021). https://doi.org/10.1016/j.scs.2021.102998
[57] L. Göransson, C. Granfeldt, A.-B. Strömberg, Management of wind power variations in electricity system investment models: a parallel computing strategy, SN Oper. Res. Forum 2 (2) (2021) 25. https://doi.org/10.1007/s43069-021-00065-0
[58] M. Wirtz, M. Heleno, H. Romberg, T. Schreiber, D. Müller, Multi-period design optimization for a 5th generation district heating and cooling network, Energy Build. 284 (2023) 112858. https://doi.org/10.1016/j.enbuild.2023.112858
[59] J. McCarty, C. Waibel, A. Schlueter, Multi-period optimisation of district-scale building integrated photovoltaic deployment, IOP Conf. Ser. Earth Environ. Sci. 1196 (1) (2023). https://doi.org/10.1088/1755-1315/1196/1/012015
[60] E. Cuisinier, C. Bourasseau, A. Ruby, P. Lemaire, B. Penz, Techno-economic planning of local energy systems through optimization models: a survey of current methods, Int. J. Energy Res. 45 (4) (2021) 4888–4931. https://doi.org/10.1002/er.6208
[61] A. Lerbinger, I. Petkov, G. Mavromatidis, C. Knoeri, Optimal decarbonization strategies for existing districts considering energy systems and retrofits, Appl. Energy 352 (2023) 121863. https://doi.org/10.1016/j.apenergy.2023.121863
[62] T. Schütz, L. Schiffer, H. Harb, M. Fuchs, D. Müller, Optimal design of energy conversion units and envelopes for residential building retrofits using a comprehensive MILP model, Appl. Energy 185 (2017) 1–15. https://doi.org/10.1016/j.apenergy.2016.10.049
[63] I. Petkov, C. Knoeri, V. Hoffmann H, The interplay of policy and energy retrofit decision-making for real estate decarbonization, Environ. Res. Infrast. Sustain. 1 (2021). https://doi.org/10.1088/2634-4505/ac3321
[64] O. Iwuanyanwu, I. Gil-Ozoudeh, A. Chukwudi Okwandu, C. Somadina Ike, Retrofitting existing buildings for sustainability: challenges and innovations, Eng. Sci. Technol. J. 5 (2024). https://doi.org/10.51594/estj.v5i8.1515
[65] P. Simpa, D. Eze Ekechukwu, The intersection of renewable energy and environmental health: advancements in sustainable solutions, Int. J. Appl. Res. Soc. Sci. (2024). https://doi.org/10.51594/ijarss.v6i6.1175
[66] M. Khairi, A. Jaapar, Y. Ziyad, The application, benefits and challenges of retrofitting the existing buildings, IOP Conf. Ser. Mati. Sci. Eng. 271 (2017). https://doi.org/10.1088/1757-899X/271/1/012030
[67] R.M. Associates, Rhino Computer software], 2007, (2025). accessed: 22-09-2025, https://www.rhino3d.com/.
[68] R.M. Associates, Grasshopper Computer software, 2007, (2025). accessed: 22-09-2025, https://www.grasshopper3d.com/.
[69] EUMETSAT, SARAH Solar Radiation, 2016, accessed: 22-09-2025, https://pvgis.com/en/sarah-solar-radiation.
[70] Swedish mapping, cadastral and Swedish, National Geodata Platform, 2024, accessed: 2025-09-12, https://www.lantmateriet.se/.
[71] Boverket, Energideklaration, 2025, accessed: 2025-09-12, https://www.boverket.se/sv/energideklaration/sok-energideklaration/.
[72] U. S. Department of Energy, Commercial reference buildings, 2025, accessed: 2025-09-12, https://www.energy.gov/eere/buildings/commercial-reference-buildings.
[73] Climate.OneBuilding.Org, Repository of Building Simulation Climate Data, 2024, accessed: 2025-04-12, https://climate.onebuilding.org/.
[74] A.f. S.E. LLC, OpenStudio [Computer software], 2008, accessed: 22-09-2025.
[75] T. Huld, Typical Meteorological Data access service [Dataset], 2017, accessed: 2025-10-30, https://data.jrc.ec.europa.eu/collection/id-0081.
[76] R. Rahmaniani, T.G. Crainic, M. Gendreau, W. Rei, The benders decomposition algorithm: a literature review, Eur. J. Oper. Res. 259 (3) (2017) 801–817. https://doi.org/10.1016/j.ejor.2016.12.005
[77] J. Bezanson, A. Edelman, S. Karpinski, V.B. Shah, Julia: a fresh approach to numerical computing, SIAM Rev. 59 (1) (2017) 65–98. https://doi.org/10.1137/141000671
[78] M. Lubin, O. Dowson, J.D. Garcia, J. Huchette, B. Legat, J.P. Vielma, JuMP 1.0: recent improvements to a modeling language for mathematical optimization, Math. Prog. Comp. 15 (3) (2023) 581–589. https://doi.org/10.1007/s12532-023-00239-3
[79] Gurobi, Gurobi Optimizer Reference Manual, 2025, accessed: 2025-05-12, https://www.gurobi.com.
[80] Sveriges riksbank, Inflationsmålet [in Swedish], 2023, accessed: 2025-09-19, https://www.riksbank.se/sv/penningpolitik/inflationsmalet/.
[81] M.R. Garey, D.S. Johnson, Computers and Intractability: A Guide to the Theory of NP-Completeness, Freeman, 27. print edition, 2009.
[82] Hemsol, Enklare energi, smartare val, 2025. In Swedish, https://hemsol.se.
[83] Solcellsofferter, Tunnfilmssolceller: Fakta, pris och information, 2025. In Swedish, https://www.solcellsofferter.se/tunnfilmssolceller/.
[84] B. Boverket, Klimatdatabas, PLXPAGE02.06.000, 2025. In Swedish, https://klimatdatabasen.boverket.se/detaljer/8/6000000203.
[85] Technical Report, Center for Sustainable Systems, Photovoltaic Energy Fact Sheet, 2024. https://css.umich.edu/publications/factsheets/energy/solar-pv-energy-factsheet.
[86] C. Mckinsey, The race to decarbonize electric-vehicle batteries, 2023. https://www.mckinsey.com/industries/automotive-and-assembly/our-insights/the-race-to-decarbonize-electric-vehicle-batteries.
[87] Rexel, Produktinformation: Elradiator, 2025. In Swedish, https://www.rexel.se.
[88] Ctc, Heat Pump-How much you can save, 2025. https://ctc-heating.com/blog/heat-pump/how-much-you-save-with-a-heat-pump.
[89] A.O. Westerberg, J. Lindahl, National Survey Report of PV Power Applications in Sweden 2023, Technical Report, Tech. rep, 2024. Swedish Energy Agency.
[90] D. Finansinspektionen, 2025. In Swedish, https://www.fi.se/sv/publicerat/statistik/diskonteringsrantekurvor/2025/diskonteringsrantekurvor-mars-2025/.